

# From macro to micro approaches in settlement archaeology: a case study of an Early Iron Age smithy at the Pungrt hillfort (Central Slovenia)

Luka Gruškvnjak<sup>1\*</sup>, Agni Prijatelj<sup>1,2\*</sup>, Petra Vojaković<sup>1,3\*</sup>, Jaka Burja<sup>4</sup>, Barbara Šetina Batič<sup>4</sup>, Rok Brajkovič<sup>5</sup>, Borut Toškan<sup>6</sup>, Tjaša Tolar<sup>6</sup>, Helena Grčman<sup>2</sup>, and Matija Črešnar<sup>1</sup>

<sup>1</sup> Centre for Interdisciplinary Research in Archaeology (CIRA), Department of Archaeology, Faculty of Arts, University of Ljubljana, SI; Luka.Gruskvnjak@ff.uni-lj.si; Petra.Vojakovic@ff.uni-lj.si

<sup>2</sup> Department of Soil and Environmental Science, Biotechnical Faculty, University of Ljubljana, SI; Agni.Prijatelj@bf.uni-lj.si  
<sup>3</sup> Arhej d. o. o., Sevnica, SI

<sup>4</sup> Institute of Metals and Technology, Ljubljana, SI

<sup>5</sup> Geological Survey of Slovenia, Ljubljana, SI

<sup>6</sup> Institute of Archaeology ZRC SAZU, Ljubljana, SI

\* corresponding author

**ABSTRACT** – *In this paper, we present an interdisciplinary and multiscalar study of an Early Iron Age smithy uncovered at the Pungrt hillfort in Central Slovenia. By examining and comparing the stratigraphic and artefactual evidence preserved at both macro- and micro-scales this study highlights the importance of integrated micromorphological and micro-refuse analyses in settlement contexts. Our integrated approach allowed us to identify the blacksmith's workshop and cyclical skimming of the floor surface in the wider area of the anvil, revealing the presence of lime plaster technology for the first time during this period in Slovenia. Additionally, we discuss the strengths and weaknesses of the macro- and micro-evidence examined, as well as the geoarchaeological methods used, by exploring the distinct ways in which micromorphology and micro-refuse analysis complement each other.*

**KEY WORDS** – *Early Iron Age; smithy; micromorphology; micro-refuse; lime floors; hammerscale; geoarchaeology*

## *Od makro k mikro pristopom v naselbinski arheologiji: študijski primer starejše železnodobne kovačnice na gradišču Pungrt (osrednja Slovenija)*

**IZVLEČEK** – *V prispevku predstavljamo večravensko interdisciplinarno študijo starejše železnodobne kovačnice, odkrite na gradišču Pungrt v osrednji Sloveniji. Študija s preučevanjem in primerjavo stratigrafske in artefaktov, ohranjenih tako na makro- kot mikroravnini, opozarja na pomen integracije mikromorfologije in analize mikro-odpada pri preučevanju naselbinskih kontekstov. Takšen pristop nam je omogočil prepoznavanje kovaške delavnice, cikličnega premazovanja tal okoli nakovala in prvič v tem obdobju v Sloveniji razkril prisotnost tehnike apnenih premazov. Poleg tega opozarjamo na prednosti in slabosti preučevanih makro- in mikro-dokazov ter razpravljam o komplementarnosti uporabljenih geoarheoloških metod.*

**KLJUČNE BESEDE** – *starejša železna doba; kovačnica; mikromorfologija; mikroodpad; apneni tlaki; škaja; geoarheologija*

## Introduction

Understanding house floors, open spaces, and activity areas is vital to household and settlement archaeology. It provides information on the architecture, organisation of the household and settlement space, and the social and economic activities that steered daily routines and interactions (e.g., Matthews 2005; Milek, Roberts 2013). These interpretative venues, however, are rarely accessible by using only traditional archaeological approaches relying on macro-observations of stratigraphic and artefactual evidence. Instead, they require an integrated micro-archaeological approach (see Weiner 2010; Milek, Roberts 2013; Milek et al. 2014). To this end, we combine soil micromorphology and micro-refuse analysis with macro-archaeological methods to examine floors and activities at one Early Iron Age smithy at the Pungrt hillfort: Building 24.

The two micro-archaeological methods offer a fine-grained resolution of distinct events and processes involved in the life cycle of individual households. As the study of archaeological deposits and (micro)stratigraphy in thin section, soil micromorphology can resolve < 0.010–5 mm thick discrete depositional units not visible to the naked eye. In doing so, it delivers unprecedented detail and temporal resolution to site formation and taphonomic processes that may range in duration from a single event to monthly, seasonal and longer timescales (Courty et al. 1989; Matthews 2017). Micro-refuse analysis can provide a key for characterising activity areas based on the reconstruction of depositional patterns of various materials and micro-artefacts, accruing, over time, across floor surfaces and reflecting distinct use-lives of the analysed space (Tani 1995; LaMotta, Schiffer 1999; Sherwood 2001). Whilst individually these techniques can produce key insights about a house (e.g., Matthews 2005; Homsey-Messer, Humkey 2016), their interpretational strength is dramatically enhanced when integrated into a multi-method dataset (e.g., Milek, Roberts 2013).

Both micro-archaeological methods, rarely employed in Iron Age hillfort research (but see Sharples 1991; Golánnová 2023; Mohammadi et al. 2023), are applied here for the first time within the hillfort and household archaeology in Slovenia (see also Prijatelić et al. 2024). In this study, we aimed to explore and compare the nature of stratigraphic and artefactual evi-

dence preserved at the macro- and micro-scales<sup>1</sup> in such contexts to assess their relative contribution to archaeological interpretation and inform future applications of such integrated methodology. The research was conducted on the Early Iron Age Building 24 and the adjacent Road 1 at the Pungrt hillfort. The stratigraphic study of architectural features and floor layer boundaries and the artefact and bone distribution analyses were compared against the results of micromorphological and micro-refuse analyses to generate new information on different architectural choices, floor construction and maintenance practices, as well as original activity areas in the building and on the street. As this paper demonstrates, it was only through this multi-scalar, multi-method approach that Building 24 was identified as a smithy.

## Pungrt hillfort

The Pungrt hillfort, situated 366 m above sea level on the eponymous hill, overlooks the small town of Ig and the southern outskirts of Ljubljana Marsh. The remains of the long-lived urban settlement, which functioned during the Iron Ages and Early Roman period, are representative of the rich, multi-period landscape found not only in the vicinity of Ig, but in the entire Ljubljana Marsh area (see Vojaković et al. 2024). The geological bedrock of the Pungrt hill consists of Lower Jurassic bioclastic limestone and dolomitized polymictic breccia. The limestone has been attributed to the Lithiotid Limestone Member of the Podbukovje Formation due to the presence of lithiotid bivalves (Dozet, Strohmenger 2000; Dozet 2009) and the dolomitized polymictic breccia to the Toarcian Breccia Member due to its superposition and geometric relationships, as it vertically intersects the underlying bioclastic limestone (Gale, Rožič 2024). The natural soils on the mostly wooded and partly meadow-covered hill include, depending on the local topography, both shallow, incipient, and thicker, more developed soil types. The former are represented by the Leptosols and Phaeozems, and the latter by Eutric Chromic Cambisols and Luvisols (see Vidic et al. 2015).

The prehistoric settlement at Pungrt covers an area of approximately 10 hectares, surrounded by a rampart that follows the topography of the hill. An additional 6 hectares to the south, enclosed by a suspected outer rampart, have not yet been examined. As a re-

<sup>1</sup> The two terms are fluid and relational. In this study, the macro-scale data encompass all the material and information gathered during the excavation at the site, while the micro-scale data include all the data obtained through geoarchaeological sampling and subsequent laboratory analyses using stereo, optical and scanning electron microscopy.

sult, the function and chronology of this area remain undetermined. The hillfort was divided into a series of man-made terraces, which were densely populated with houses arranged in parallel rows (Fig. 1). The urban settlement was occupied, apparently continuously, for 10 centuries from the 8th/7th century BC to the 2nd century AD (see *Vojaković et al. 2024*).

### Building 24: from macro to micro evidence

Building 24 was one of the best preserved among a group of 50 that were excavated at the site during the development-led excavation in 2020–2021. Situated on the first, relatively flat and spacious terrace with deep stratigraphy, it was also one of the 14 buildings, sited adjacent to the 2m-wide Road 1. The latter ran along the inner face of the monumental stone rampart (Fig. 1) and consisted of muddy deposits interfingered with either gravelly or pebbly material.

Building 24, similar to the other Iron Age structures on the first terrace, was rebuilt several times on the same building-stance. Over the course of some 400 years (8th/7th–4th centuries BC), its complex Early and Late Hallstatt developmental sequence (Phases I and II) saw it rebuilt four times, with the consecutive buildings

retaining the same position and orientation. It was abandoned sometime in the Late Iron Age (Phase III) or the Early Roman period (Phase IV), without any evidence of a catastrophic event, such as destruction by fire. In its place, a thick dark anthropogenic soil (*i.e.* Dark Earth; see *e.g.*, *Howard 2017*) developed, suggesting a significant change in land use in this area of the settlement, probably associated with some form of agriculture. The latter has also been attested for this area in both the stratigraphic sequence and the historical sources for the Modern period (Phase V).

### Macro-stratigraphic evidence

Excavation, following procedures described in Gruškovič *et al.* (2025), revealed that during its Late Hallstatt Phase IIb2 – examined in this paper – Building 24 (Fig. 2) had dry-stone foundations (stratigraphic units, henceforth SU 2049=2055, 2092), 50cm wide and 40cm high, built with stones, 25 to 80cm in size, arranged in a single or double row. The southern foundation was preserved to a length of 5.5m, the northern to 5m.

The limestone foundations of the walls, which do not exceed a distance of 6m, and the absence of pits for



**Fig. 1. Pungrt hillfort. Late Hallstatt period composite plan of the excavated area (figure by P. Vojaković).**

post holes in the interior of the building, indicate a timber-framed construction, characterized by the beams connected by cross-jointing at the corners (Črešnar 2007.16–18; Dular 2008.341; Vojaković 2013.305–306). While no timber was preserved in relation to Building 24, a long piece of the charred square beam was recorded for Building 2, confirming the existence of timber-framed buildings on the site, which were also evidenced by daub fragments with wood impressions uncovered throughout the site.

The stone foundations were thus the only elements of standing architecture preserved and available for macroscopic analysis. The lithofacies types the stones belong to were classified according to the updated

Dunham classification (Lokier, Al Junabi 2016), while the shaping of the stone was assessed according to the criteria in Petra Žvab Rožič *et al.* (2022).

The variety of lithofacies types employed for the stone foundations included Bivalve Floatstone, Lithiotid Floatstone to Rudstone, Oncoid Cortoid Packstone and several fine-grained limestone lithofacies (Carbonate Mudstone with rare fossils, Peloid Wackestone). The former are indicative of the Lithiotid Limestone Member (according to Gale 2015 and Djurić *et al.* 2022), while their biostratigraphic age can be assigned based on the presence of lithiotid bivalves to the upper part of the Lower Jurassic (Pliensbachian) (Buser, Debeljak 1997). As the local presence of this limestone is con-

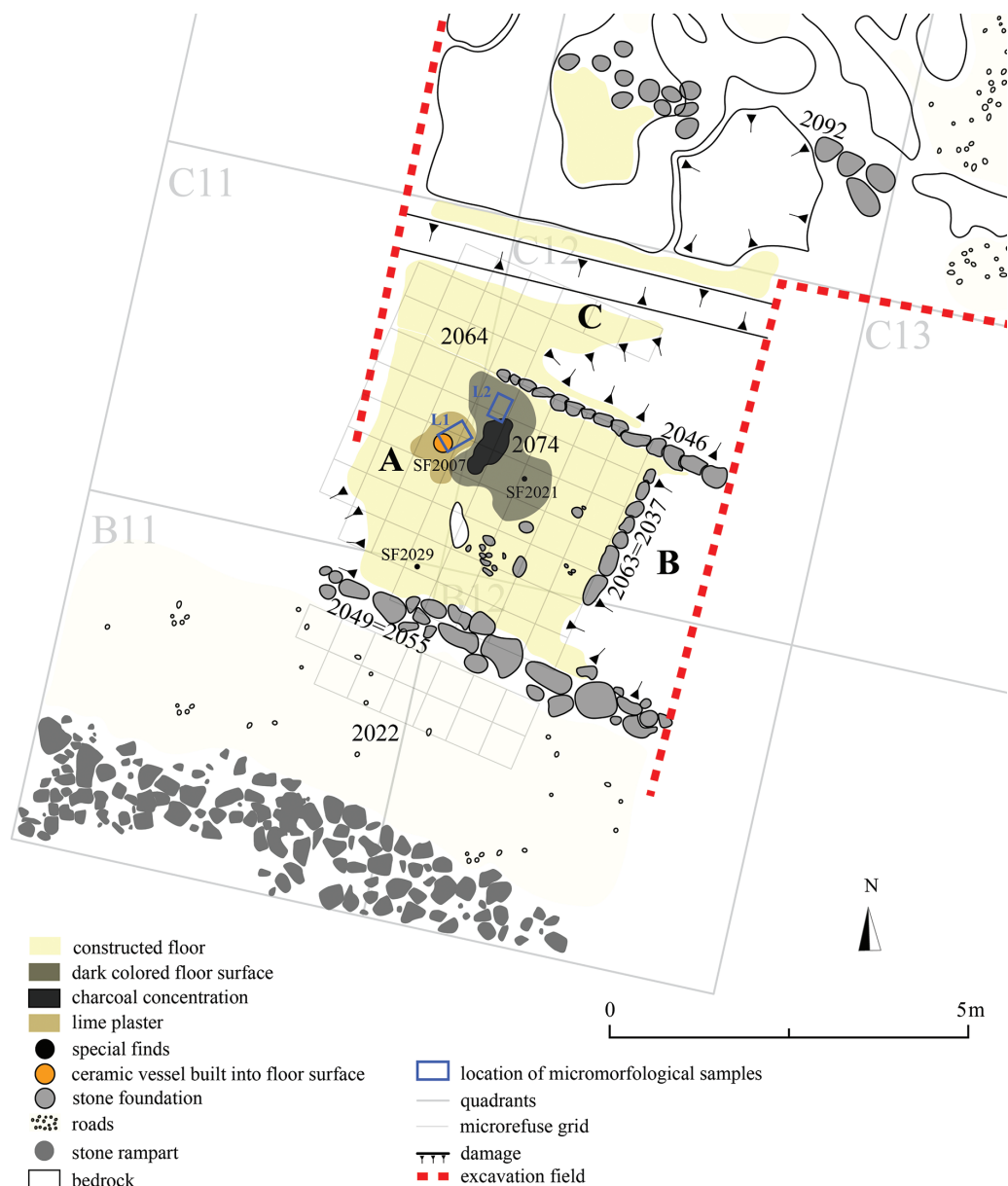


Fig. 2. Pungrt hillfort. Plan of the Late Hallstatt period Building 24 in the IIb2 phase (figure by P. Vojaković).

firmed by a geological map (*Djuric et al. 2022. Fig. 20*), it is reasonable to assume that the stone blocks used were extracted locally.

The foundation walls were only roughly shaped. The select surfaces of stone blocks would have been worked, as evidenced by their shape, which in several cases had perfectly square chiselled edges. An almost flat surface that has been smoothed with only minor chipping was observed in the outer wall faces. The overall rough shape of the studied limestone blocks indicates that only a low-level of stonemasonry skill was employed in the building's construction.

The interior of the building was divided into three distinct areas, which had been separated by partition walls, again erected on dry-stone foundations (SU 2046, SU 2063=2037/2038), albeit in this instance, only up to 30cm wide and constructed of individual stones up to 40cm in size. The two smaller rooms (*i.e.* Rooms A and B) were located at the southern end of the building, while the third, large room (*i.e.* Room C) occupied the entire northern end. In the south-western Room A, with an excavated area of *c.* 10m<sup>2</sup>, the occupation surface was easy to trace due to the presence of a constructed yellowish-brown silty clay floor (SU 2064.1), which was up to 9cm thick. The same floor continued into the largest, northern Room C (*c.* 20m<sup>2</sup>), where it was preserved only in traces due to the presence of a rocky outcrop and extensive later disturbances. No floor evidence was preserved or discerned in the smallest, south-eastern Room B (*c.* 3m<sup>2</sup>).

Whereas no constructed hearths were recorded in any of the three rooms, an oval patch (1×0.4m) composed of finely comminuted charcoal (SU 2074) was identified in the centre of Room A. To the west of this feature, a ceramic vessel (special find, henceforth SF 2007) was set in a pit (SU 2089/2090) within the floor. The pit and the floor immediately around it were covered with a pinkish-white material of a coarser-grained, silty clay loam texture (SU 2064.3), which micromorphology has shown to be a clay lime plaster (see below). At the contact with the vessel this plaster and pit infill both appeared rubified, indicating that high temperatures were present in the vessel. In addition, the plaster contained aggregates of the same clay lime material, some of them with rubified contact surfaces similar to the *in situ* contact with the vessel (*Gruškovnjak et al. 2024.2.2. Ig 94*), indicating a previous episode of removing the vessel and installing it anew.

After the end of the building's life cycle in phase IIb2 it seems to have been immediately followed by the construction of a new building above the previous one (Building 24, Phase IIc1).

### **Micro-stratigraphic evidence**

Four undisturbed block samples for micromorphological analysis were taken at two locations within Room A, targeting the patch of the pinkish-white silty clay loam surrounding the ceramic vessel set into the floor (Location 1) and the dark-coloured part of the floor at the northern end (Location 2), where its surface appeared somewhat drier and harder, suggesting thermal alterations in this area (Fig. 2). In addition, four monoliths for control samples were extracted from the natural subsoil underlying the archaeological sequence on the Terrace 1 (Fig. 1). The sampling and thin section preparation followed the procedures described in Luka Gruškovnjak *et al.* (2025) and the micromorphological descriptions followed the terminology used in Georges Stoops (2021), with reference to additional texts such as Panagiotis Karkanas and Paul Goldberg (2019), and Cristiano Nicosia and Georges Stoops (2017). Distinct micro-layers distinguished within the macroscopically documented stratigraphic units were given a number suffix (*e.g.*, SU 2064.3–2064.9) and described separately (see Tab. 1).

### **Micro-stratigraphic floor sequence**

The micromorphological analysis (Tab. 1) of floor samples from the building revealed a combination of a preparation layer (SU 2071) and an overlying constructed, silty clay floor (SU 2064.1) (Figs. 3, 4.A–D; *Gruškovnjak et al. 2024.2.3. Figs. 2–3*). At the microscopic level, the two differed in their heterogeneity, internal fabric, texture, porosity and inclusions. The examined preparation substrate (SU 2071) consisted of a mixture of loose occupational debris (charcoal, bone, pottery), remnants of old floors, their plasters, finishing coats and other construction materials, as well as coarser carbonate clasts, all chaotically distributed within the layer. Compared to the constructed floor, the matrix of the construction fill was coarser-grained (silty clay loam) and more carbonate-, organic- and phosphate-rich due to the larger quantity of carbonate grains, charcoal, humified plant material and post-depositionally formed phosphate nodules. The nature of the material suggests that SU 2071 was a mixture of indoor and outdoor, occupational and demolition debris. This heterogeneous material would have been employed as a levelling substrate for the overlying

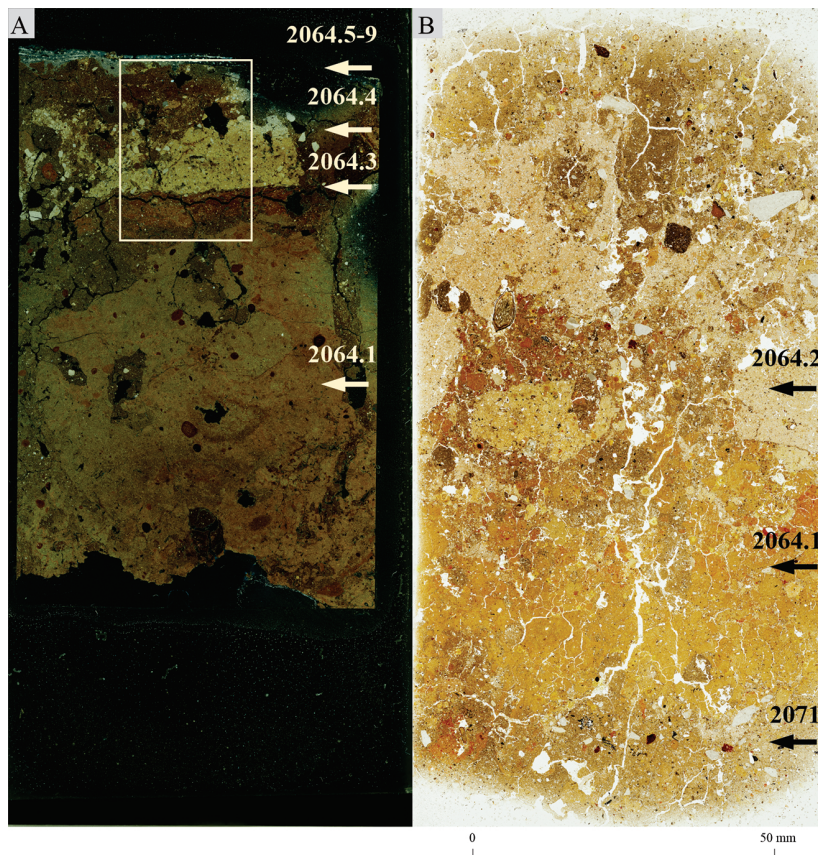


**Fig. 3. Pungrt hillfort.** A couple of floor (micro)stratigraphic sequences captured in micromorphological blocks Ig 3 at Location 2 and Ig 5 at Location 1 within Building 24, which are associated with its IIb2 phase. The sequence in Ig 3 (A, in XPL) includes (from bottom to top): a constructed, silty clay floor (SU 2064.1), and a series of alternating earthen and lime-based floor coats and washes (SUs 2064.3 – 2064.9), with the higher magnification image of the latter provided in Figure 5. The sequence in Ig 5 (B, in PPL) includes (from bottom to top): a preparation layer (SU 2071), a constructed, silty clay floor (SU 2064.1), and a lime plaster (SU 2064.2) (figure by A. Prijatelj).

constructed floor (SU 2064.1). In contrast to the latter, it exhibited greater porosity and no signs of wetting, kneading and pugging, suggesting that it was deposited across the construction area in a dry state.

A combination of macro- and micro-characteristics, including its field geometry, the compacted nature of the matrix, the homogeneity of the fabric and the sharp upper and lower contacts of SU 2064.1 were consistent with a constructed floor. A comparison between control soil samples (Ig 1811, 1813) and the analysed deposit demonstrated a similarity between the two types of groundmass identified within SU 2064.1 and B horizons at the site, which, at the microscopic scale, vary in their clay content (Tab. 1; *Gruškovič et al. 2024.2.3.Fig. 1*). The raw material for the silty clay floor would have been procured locally from the carbonate-free, clay-rich B horizons, located in the areas with deeper and more developed soil types (*i.e.* Eutric Chromic Cambisols and Luvisols). As the naturally existing differences between clay-rich and clay-poorer areas within the local B horizons continued to be present also within the groundmass of the constructed floor, it appears that the wetted material would have been kneaded and pugged, without being thoroughly homogenized, thus preserving the naturally occurring variations in clay content of the local subsoils within the

floor itself (Fig. 4.C-D; *Gruškovič et al. 2024.2.3.Fig. 3.A-D*). When applied across the levelling fill in a wet state, parallel arrays of vesicles and smooth vughs (*Gruškovič et al. 2024.2.3.Fig. 3.E-F*) would have been produced by water or air escaping from the construction material during the drying stage, which would have probably taken place over the course of several days (*Karkanas 2018; Goldberg 2019.129; García-Suárez et al. 2021*).

The yellowish-brown silty clay floor (SU 2064.1) was treated differently in different areas of Room A. The three types of floor covering – plasters, finishing coats and washes – were distinguished based on their thickness, as observed in thin sections (Tab. 1, Figs. 3.A, 5, 6). More specifically, the clay lime plaster (SU 2064.2) was some 65mm thick, finishing coats (SUs 2064.3–2064.7, 2064.9) ranged from 3.5 to 14mm in their thickness, and the single lime wash (SU 2064.8) was, at 0.5mm, the thinnest among the identified floor coverings.

The thick clay lime plaster (SU 2064.2) covered the yellowish-brown silty clay floor in the area surrounding the ceramic vessel (SF 2007) built into the floor in Room A (Location 1, Figs. 3.B, 4.E–F; *Gruškovič et al. 2024.2.3.Fig. 4*). The deposit was identified as containing lime due to the nature of its binding matrix and

Location	(Micro) Stratigr. Unit	Micromorphological Description	Interpretation
Building 24, Room A, Location 1	Terrace 1	Control subsoil samples	Micromorphological Description
		Ig 1808, 1811, 1813, 1815	Yellow to reddish yellow silty clay with moderate porosity (5-10%) and no carbonate grains. Trace amounts of silt-sized microcharcoal (< 1%), occasional iron-manganese nodules (2-5%), and occasional intact and fragmented clay coatings (2-5%), the quantity of which increases with depth.
	2064.2	Ig 5, 94	A dense layer of pinkish white to pink silty clay loam, which is progressively rubefied to reddish yellow towards the top. The micromass is composed of a mixture of micrite and clay. Carbonate aggregate within the micromass consists of moderately sorted subangular, subrounded and rounded grains in fine and medium sand fractions (40%). Few lime lumps (5%), few humified plant fragments (2%), trace amount of charcoal (< 1%), rare Fe-Mn (hydr)oxide coatings (< 2%) and clayey phosphate nodules (< 2%) are all present within the deposit.
	2064.1	Ig 5	Reddish yellow silty clay with occasional relict iron-manganese (hydr)oxide nodules (2%) and trace amounts of silt-sized microcharcoal (< 1%), evenly dispersed through the matrix. Within the dense groundmass, commonly disrupted by channels and chambers (15-20%), are embedded very few clay lime plaster aggregates (3%), rubified silty clay aggregates (< 2%), and clayey phosphate nodules and infillings (< 2%).
	2071	Ig 5	Moderately to very porous (16-30%), aggregated, organic-rich, yellowish brown to dark brown silty clay loam with few gravel-sized carbonate clasts (5-15%) and common anthropogenic inclusions (16-25%): macro and micro charred plant remains, bone and pottery fragments, fragments of old floors, their plasters, finishing coats, burnt and unburnt aggregates of pure clay, and phosphate nodules and vivianite.
	2064.9	Ig 3	Yellowish red to red silty clay loam with few relict iron-manganese (hydr)oxide nodules (5%). Sub-horizontal planar voids in the upper part of the layer.
	2064.8	Ig 3	A thin, pinkish white lense of carbonate-rich aggregates and quartz sand.
	2064.7	Ig 3	Yellowish red to red silty clay loam with few relict iron-manganese (hydr)oxide nodules (5%).

**Tab. 1. Pungrt hillfort. Summary micromorphological description of deposits from Building 24 in its IIb2 phase (figure by A. Prijatelj).**

Building 24, Room A, Location 2	2064.5	lg 3, 4	Carbonate-rich reddish yellow lamina with texture, fabric, microstructure and individual components similar to SU 2064.4.	A 5,5mm thick clay lime floor coat, produced with dry slaking, and applied across the floor surface in the N section of Room A. The rubefaction of the coat suggests increased temperatures on the floor surface.
	2064.5	lg 3, 4	Yellowish red to red silty clay loam with few relict iron-manganese (hydr)oxide nodules (5%), evenly dispersed trace amounts of silt-sized microcharcoal (< 1%) and charred fibrous plant fragments (< 1%), as well as few aggregates of rip-up clasts from the underlying SU 2064.4 (2%) and aggregates of other, clay-based construction materials (1%).	A 14mm thick earthen floor coat with silty clay loam texture, and (probably unintentional) addition of rare plant fibers, applied across the floor in the N section of Room C. The rubefaction of the coat suggests increased temperatures on the floor surface.
	2064.4	lg 3, 4	A dense layer of pink to yellow silty clay loam, with the micromass composed of a mixture of micrite and clay. Carbonate aggregate within the micromass consists of moderately sorted subangular, subrounded and rounded grains in fine and medium sand fractions (40%). Few lime lumps (5%), few humified plant fragments (2%), trace amount of charcoal (< 1%), and occasional clayey phosphate nodules and infillings (3%) all present within the deposit.	A 12.5mm thick clay lime floor coat, produced with dry slaking, and applied across the floor area in the N section of Room C.
	2064.3	lg 3, 4	Pure red clay, rich in quartz sand (15-25%). A dense, poreless microstructure post-depositionally disturbed by channels and vughs. The clay groundmass has a random-striated birefringence fabric. On the upper surface is a thin lens (0,01mm) of comminuted, horizontally oriented charred plant remains.	A 11mm thick, earthen floor coat made of pure red clay mixed with quartz sand. Applied across the silty clay floor in the N section of Room A. Its ritual significance perhaps associated with the inauguration of the smithy. A thin layer of soot on the surface suggests a proximity of a combustion feature.
	2064.1	lg 3, 4	See description for the SU at Location 1. Notably, at Location 2, no inclusions of clay lime plaster and rubified silty clay aggregates, nor clayey phosphate nodules and infillings were identified in the layer.	See description for the SU at Location 1. At location 2, the reddish yellow silty clay floor appears to be less damaged by the bioturbation compared to Location 1.
	2071	lg 4	See description for the SU at Location 1.	See description for the SU at Location 1.

**Tab. 1. Continued**

the presence of half-burnt carbonate clasts and lime lumps (see also *Karkanas 2007*). Within the plaster, the heated carbonate clasts appeared to become progressively brown, developing complex shrinkage fracture patterns and rims of a reacted lime (*Gruškovnjak et al. 2024.2.3.Fig. 4.C*). Having several possible origins, including unreacted, half-reacted and overburnt quicklime, as well as crudely slaked lime (*Leslie, Hughes 2002*), lime lumps represented one of the defining features of the analysed lime plaster. In thin sections, they were recognized as grey, sand-sized carbonized lime aggregates of micrite with a diffuse halo gradually blending into the matrix (*Gruškovnjak et al. 2024.2.3.Fig. 4.D*). The latter had a hazy, pixelated appearance, with calcite crystallites sharing interconnected boundaries and forming a continuum within the matrix (*Gruškovnjak et al. 2024.2.3.Fig. 4.E-F*). This characteristic of lime micromass is, in fact, a fundamental property that allows discerning between the lime and the carbonate-rich, clayey materials, in which micrite grains are, as a rule, individually embedded within the clayey matrix (*Karkanas 2007.786-*

787

. Rather than pure lime, the material employed for SU 2064.3 was clay lime: the presence of clay, quartz and mica grains and iron-manganese (hydr)oxide nodules within the matrix suggests that the damp mineral subsoil was mixed with the carbonate aggregate and lime binder in the process of hot mixing or dry slaking (see also *Prijatelj, Gruškovnjak 2023*). The progressive reddening of the material towards the top of the layer (*Gruškovnjak et al. 2024.2.3.Fig. 4.A-B*) indicates that this floor area would have been exposed to high temperatures.

At Location 2, the silty clay floor was periodically coated with alternating thin, earth- and lime-based finishing coats and washes, which created an intricate microstratigraphic sequence of seven micro-layers (SUs 2064.3-2064.9) on top of the constructed floor (Tab. 1, Figs. 3.A, 5, 6). Three different types of raw materials were employed for skimming the floor surface: while the earliest, some 11mm thick SU 2064.3 consisted of pure red clay mixed with quartz sand, the subsequent, progressively thinner coats SUs 2064.4-2064.9 were

alternately made of coarser textured, silty clay loam, and clay lime. In one particular instance (SU 2064.5), the earth-based finishing coat also contained a probably unintentional addition of a few plant fibres that were charred (Fig. 6.C). Rotational features identified

in the same micro-stratigraphic unit might have been associated with the kneading, pugging or the directional pressure in the application of this finishing coat (Gruškovič et al. 2024.2,3, Fig. 5.E–F; see also Karakanas 2018). Sub-horizontal planar voids in SU 2064.7,

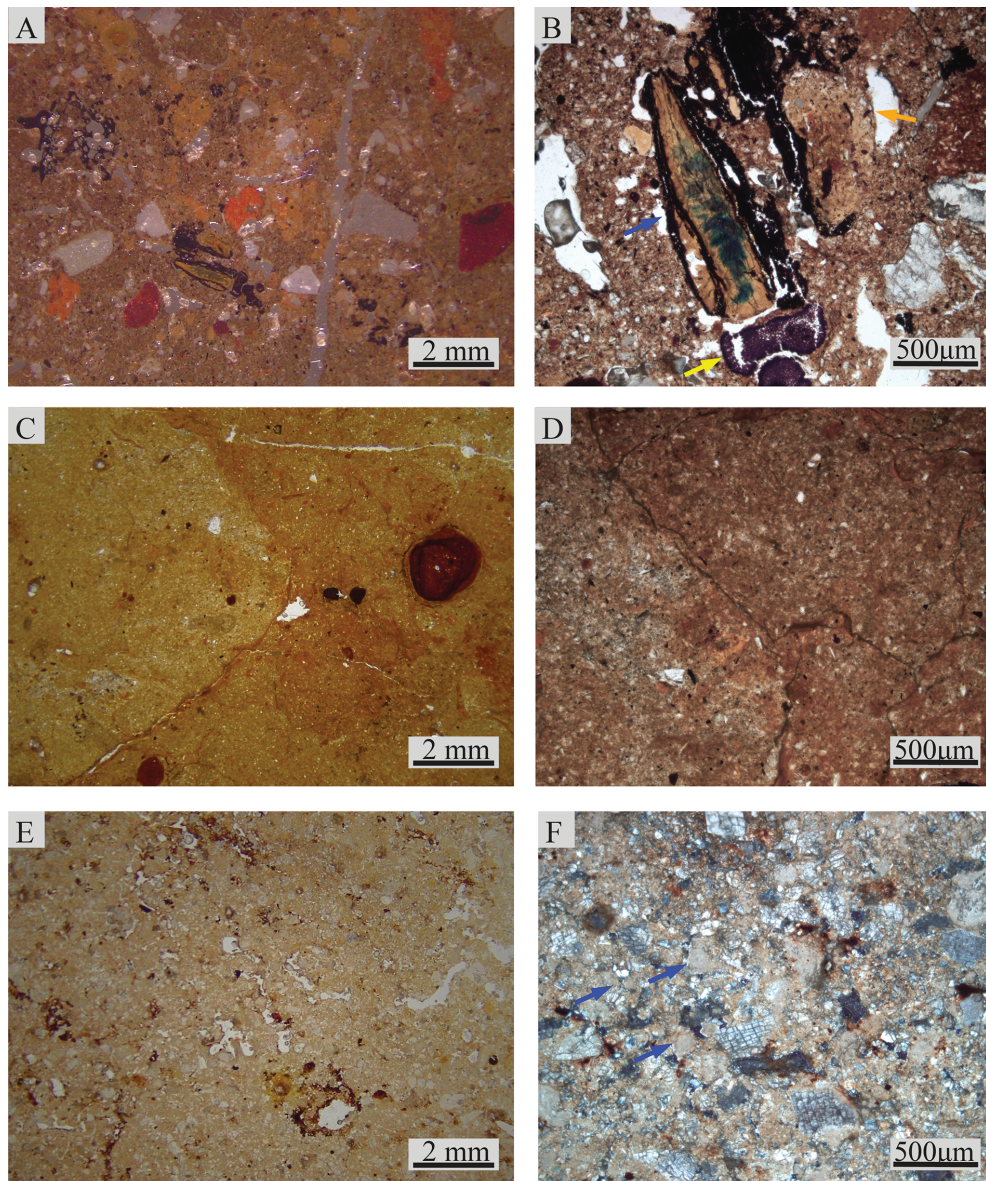


**Fig. 4. Pungrt hillfort. Photomicrographs of stratigraphic units within Building 24 in its IIb2 phase:** A a preparation layer SU 2071 consisting of the silty clay loam with heterogeneous anthropogenic inclusions, such as charcoal, aggregates of various construction materials, and pure clay (Ig 5, OIL); B the presence of sclerotia (yellow arrow, bottom of the image), and vivianite (blue arrow, centre left) and phosphate nodules (orange arrow, centre right), frequently associated with the in situ decay of charred and humified plant material indicates that the preparation layer SU 2071 is organic-rich (Ig 5, PPL); C–D constructed, silty clay floor (SU 2064.1) with variations in clay content within its groundmass (compare left and right side of the image), which suggest that the material procured from the local subsoils was not thoroughly homogenized during the preparation process (Ig 3, PPL); E lime plaster (SU 2064.2) with a silty clay loam texture and rare Fe-Mn (hydr)oxide coatings and clayey phosphate nodules (Ig 5, PPL); F the micromass of the lime plaster (SU 2064.2) is composed of a mixture of micrite and clay; note the carbonate aggregate in fine and medium sand fractions, and few lime lumps (blue arrows), recognizable due to their diffuse boundaries with the surrounding matrix (Ig 5, XPL) (figure by A. Prijatelj).

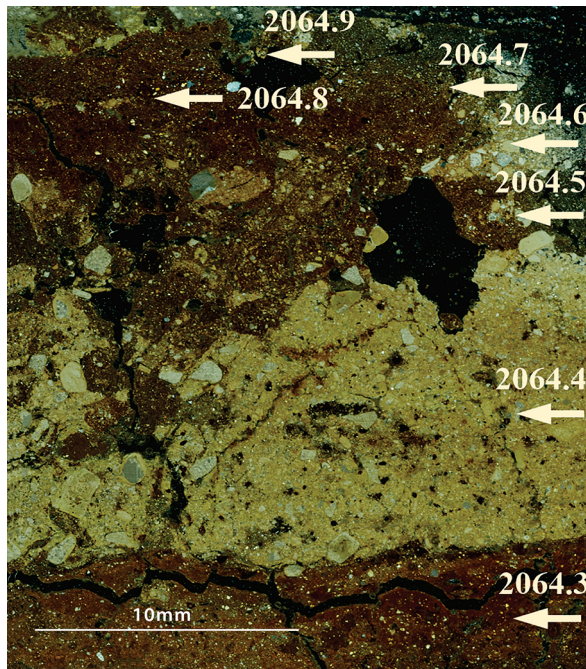


**Fig. 5. Pungrt hillfort.** A series of alternating earthen- and lime-based floor coats and washes (SUs 2064.3 – 2064.9) overlying the constructed, silty clay floor (SU 2064.1) at Location 2 (Ig 3, XPL) within Building 24 (phase IIb2). The sequence includes (from bottom to top): a 11mm thick earthen coat made of pure red clay mixed with quartz sand (SU 2064.3), a 12.5mm thick lime coat (SU 2064.4), a 14mm thick, earthen, silty clay loam coat with addition of plant stabilisers (SU 2064.5), a 5.5mm thick lime coat (SU 2064.6), a 3.5mm thick earthen, silty clay loam coat (SU 2064.7), a 0.5mm thick lime wash (SU 2064.8), and a 2mm thick, earthen, silty clay loam coat (SU 2064.9) (figure by A. Prijatej).

on the other hand, suggested intense trampling in the area that caused cracking of the material. Significantly, all of the identified finishing coats in this area appeared rubified, which suggests they were altered by high temperatures (Tab. 2, Fig. 6).

#### Macro-artefact evidence

Altogether, 320 ceramic, metal, and bone macro-finds were recovered from Phase IIb2 occupation surfaces within Building 24 and from Road 1 in front of it (Tab. 2). The area of 50m<sup>2</sup> was spread over 6 quadrants, 5×5m in size (Fig. 2). The finds were recovered from two different stratigraphic units, including the floor within the building (SU 2064) and the muddy deposits on Road 1 (SU 2022) (see Gruškovič et al. 2024, 3.).

#### Macro-artefact chronology

Of 174 macro-artefacts recovered from Phase IIb2 occupation surfaces within Building 24, only a few (n=16)

could be typologically classified. The most numerous were pots (Fig. 7.1 and 3–4), followed by tripods (Fig. 7.8) and baking lids (Fig. 7.5–6 and 9). A situla and a ciborium (high-legged vessels) (Fig. 7.2 and 7) as well as the bottom of the vessel, which has a knob inside (Fig. 7.11) were represented by one specimen each.

The dating of the pottery assemblage is difficult due to the temporal insensitivity of the forms and the lack of decoration. The most precisely datable pieces are the fragments of a situla and a ciborium found in Room A. The fragment of the situla (Fig. 7.2) was classified as a footless situla of version Ib1 according to Snežana Tecco Hvala (2014, 329, Fig. 2.9–10). This type of situla has been known only from a few graves at Križna gora in the Notranjska region, dated to the 9th–8th century BC (Urleb 1974, Tab. 1:1–3, 3:17–26, 8:1–7; Guštin 1973, 469, Fig. 2; 1979, 25, Fig. 9). The ciborium leg fragment (Fig. 7.2 and 7) is more difficult to identify, but the oxidising atmosphere during firing suggests that it is a younger form. They appear relatively early (8th century BC) in the Dolenjska region. However, such vessels increased in number in the following phases (7th–6th century BC) and continued to be used throughout the Early Iron Age. The shapes of the ciboria are very varied and have no parallel outside the Dolenjska region, which indicates that the vessels were made based on local designs in local workshops (Dular 1982, 54).

A narrower and more secure *post quem* date was provided by the two fibulae recovered from the levelling deposit (SU 2071). The first fragment of a bronze three-knobbed fibula (SF 2030; Fig. 7.15) belonged to Type

MATERIAL GROUPS	FUNCTIONAL GROUPS	FORMS
CERAMIC	Cooking ware	Pot
		Tripod
		Ciborium
		Situla
	Table ware	Lid
		Baking lid
		Ceramic ring
		Platter
		Portable oven
	Cooking utensils	Firedog
		Tools
		Tuyere
	Building material	Burnt clay
METAL	Bronze	Unidentified

**Tab. 2. Pungrt hillfort.** A representation of material groups, functional groups and forms of macro-artefacts discovered within Building 24 and on Road 1 in the IIb2 phase (figure by P. Vojaković).

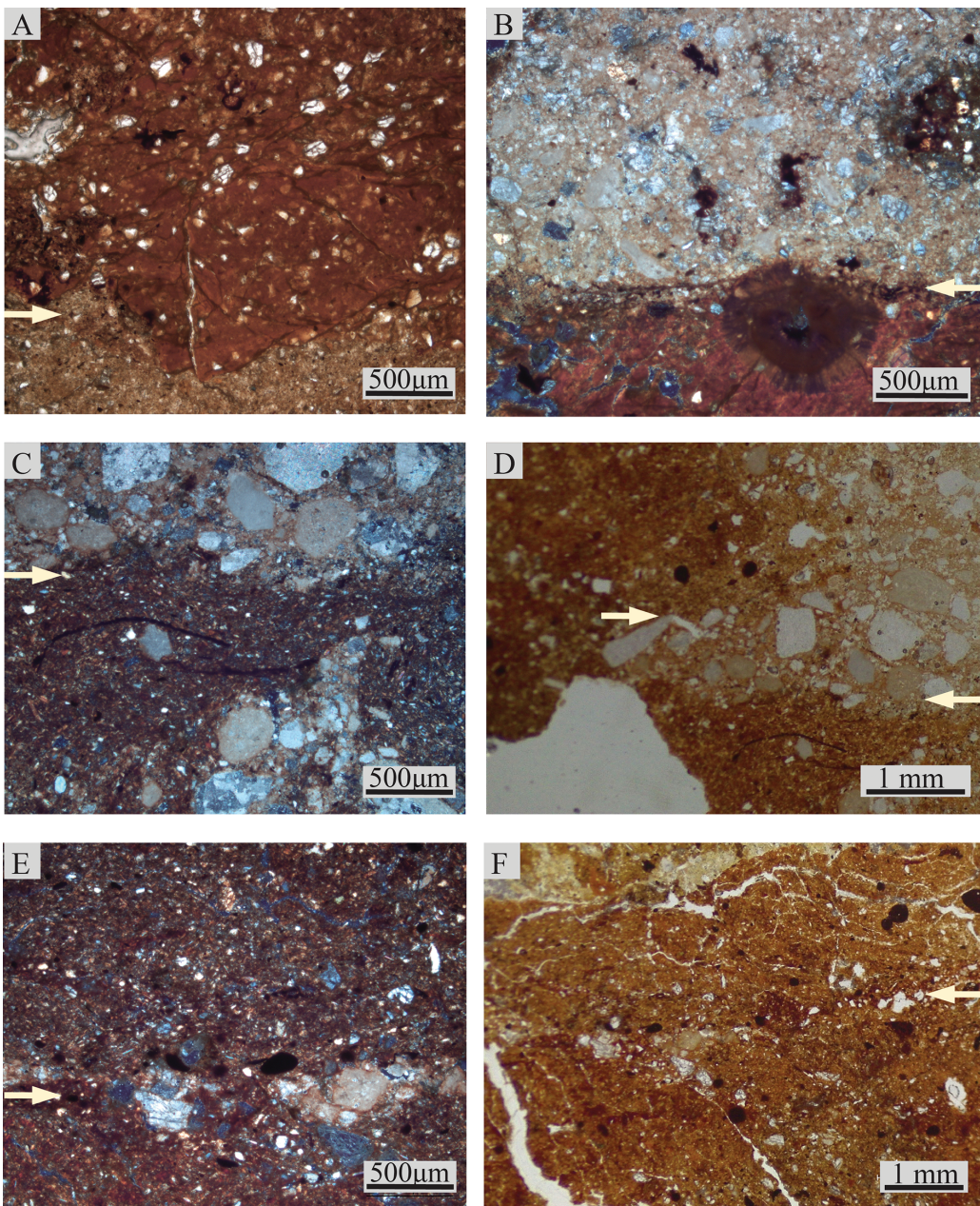


**Fig. 6. Pungrt hillfort. Photomicrographs of microstratigraphic units captured at Location 2 (Ig 3) within Building 24 in its IIb2 phase:** A a sharp and undulating contact between the constructed, silty clay floor (SU 2064.1) and the overlying pure red clay floor coat with quartz sand mixed in (SU 2064.3); the non-linear contact suggests the application of the red clay coat at the time when the silty clay floor was constructed (PPL); B a sharp and linear contact between the red clay floor coat (SU 2064.3) and the overlying lime floor coat (SU 2064.4); note a thin layer of soot on top of the clay coat, suggesting the proximity of the combustion feature and the passage of time prior to the application of the overlying lime coat (XPL); C a sharp and sub-horizontal contact between the earthen floor coat (SU 2064.5) and the overlying lime coat (SU 2064.6); the earthen floor coat (SU 2064.5) with silty clay loam texture has a probably unintentional addition of few plant fragments, and a few aggregates of rip-up lime clasts from the underlying SU 2064.4 (bottom of the image) (XPL); D a sharp and sub-horizontal contact between the earthen floor coat (SU 2064.5) and the lime floor coat (SU 2064.6) (lower arrow), and a clear and sub-horizontal contact between the lime floor coat (SU 2064.6) and earthen floor coat (SU 2064.7) (upper arrow, PPL); E a 0.5 mm thick lime wash (SU 2064.8) applied across the earthen floor coat (SU 2064.7); note a few microcharcoal fragments on the surface of the lime wash, suggesting the proximity of the combustion feature and the passage of time prior to the application of the overlying earthen floor coat (XPL); F the earthen floor coat with a network of sub-horizontal planar voids, suggesting regular traffic and trampling in the area (PPL) (figure by A. Prijatelj).

VII after *Ogrin* (1998.113,115, Fig. 15). Such fibulae were mainly characteristic for 6<sup>th</sup>-mid-4<sup>th</sup> century BC. They often appeared together with small long-footed fibulae with a reticular decorated bow (*Teržan, Trampuž* 1973.429–430, Fig. 4. 2). A fragment of such a fibula (SF 2032; Fig. 7.16) was also found on the same levelling deposit (SU 2071). This suggests that the IIb2 phase of building 24 can hardly be older than the late 6<sup>th</sup> century BC.

### Macro-artefact patterning

Comparing the density of macro finds per m<sup>2</sup> between the building's interior and the adjacent road showed significantly higher densities on the road compared to the building (Fig. 8.A). Cooking ware and burnt clay were the most abundant both inside and outside the building, but their numbers were significantly higher

on the road surface. There they are followed by cooking utensils and animal bones, which were again more abundant on the road compared to the building. On the contrary, tableware was poorly represented on the road but was relatively abundant in the building. Similarly, there were also more bronze fragments discovered in the building's interior.

The significantly higher densities of most finds on the road in front of the building could, on the one hand, be mainly related to removing waste produced within the building and depositing it on the road in front of it (see *Hayden, Cannon* 1983.125,139–140; *Deal* 1985.260–261; *Tani* 1995.237; *Sherwood* et al. 1995.453; *LaMotta, Schiffer* 1999.21–22). However, it might also (partly) represent deliberate addition of coarse material to aid runoff (*Rosen* 1989.566, 573; *Raja, Sindbæk* 2020.179).

Tableware perhaps represents a more valuable type of pottery which was treated and disposed of differently, perhaps as provisional refuse intended for reuse (see *Hayden, Cannon* 1983.130–131; *Tani* 1995.240), while bronze fragments (Fig. 7.12) most likely represent remains of small unintentionally lost objects (see *Fehon, Scholtz* 1978; *Hayden, Cannon* 1983.160).

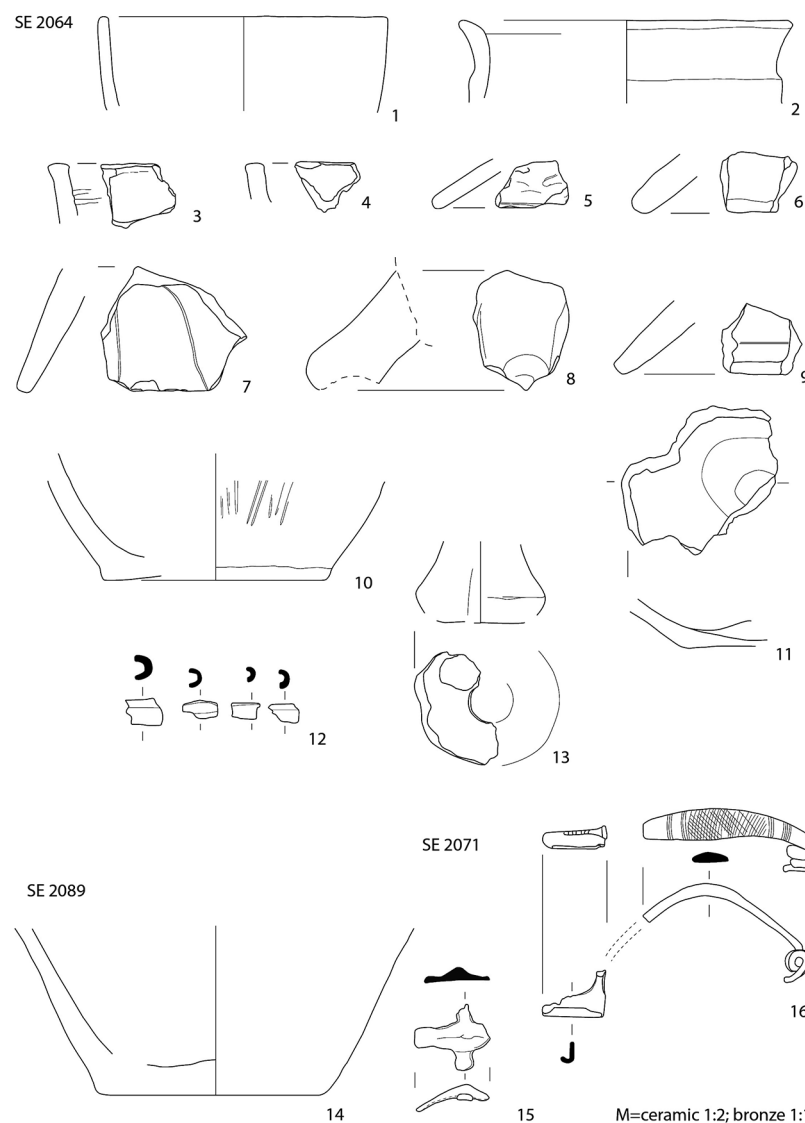


**Fig. 7. Pungrt hillfort. Representative macro-finds from Building 24 in the IIb2 phase (figure by P. Vojaković).**

The coarse excavation grid (5×5m) used for basic spatial reference of finds during fieldwork does not allow for any detailed observations of artefact patterning across the building's interior. Virtually all finds were documented in the western area of the building (in quadrant C11; Fig. 8.B), where the passageway between Rooms A and C was located. In this area within Room A, the vessel built into the floor (SF 2007=SU 2089; n=84; Fig. 7.14) was located. Compared to the reddish-brown colour of the vessel the base in its interior was very dark brown. This colour is not the result of charred food remains but instead indicates the storage of some substance, which has caused the colouring of the base and lower part of the vessel.

A concentration of burnt clay was discovered between the vessel and the charcoal layer (SU 2074). Not a single specimen of burnt clay displayed any wood impressions, which would (undoubtedly) identify them as the remains of burnt daub. Therefore, we assume that the fragments likely belonged to a portable hearth, oven or furnace used in this area. The predominance of cooking ware, cooking utensils and tableware among the macro-artefacts in the building would lead us – without the additional microarchaeological methods employed – to the conclusion that domestic activities of food preparation and serving were dominant in its interior.

However, the high density of burnt clay along with a putative tuyere (SF 2029; Fig. 7.13) could be related to remains of a high-temperature fire installation such as a smelting furnace or a forge hearth (e.g., *Eliyahu-Behar et al. 2012; Workman et al. 2021*). In this case, they could suggest that some metallurgy-related craft activities have taken place in Room A. In addition, the 5 small fragments of a bronze tubular object (SF 2021; Fig. 7.12) might be attributed to an accidental loss of an object that would have been part of a personal attire or equipment. In light of the possible craft activities in the building (see below), it is important to note that the tiny artefact (Fig. 7.12) might have already been lost during its manufacturing stage (see *Fehon, Scholtz 1978.272*).

Similarly to the cooking ware, animal bones were also represented in much higher densities on the road compared to the building's interior. In terms of species (Fig. 9.A), cattle (*Bos taurus*) bones are the most abundant in both assemblages, followed by sheep or goat (*Ovis aries* / *Capra hircus*) bones on the road. Interestingly, the domestic pig (*Sus cf. domesticus*) is poorly represented only in the road assemblage while the probable wild boar (*Sus cf. scrofa*), possibly the only wild species represented, was discovered in the building. It was

the above-average size of the specimen that suggested a wild (rather than domestic) pig, although in principle, it could also be an atypically large male domestic pig or a hybrid.

From the meat quality perspective (after *Uerpmann 1973; Fig. 9.B*), bones from medium-quality and low-quality meat body parts dominate the assemblage on the road, while high-quality and low-quality parts dominate the building's interior. However, the assemblage from the building is too small to draw conclusions. In general, the analysed bone assemblages, show no clear signs of selection in favour of certain parts of the carcass and, in this sense, no specialized activities associated with the particular phase of the meat processing *chaîne opératoire* (see e.g., *Seetah 2019*). Nevertheless, the pattern of fragmentation of the long bones suggests that fresh bones would have been broken to access marrow (e.g., bovine humerus and metatarsus). Exceptionally, a macro bone fragment showed irregular fractures with a roughened surface of the compact at the fracture site, a feature usually associated with the breaking of old, largely dried bone (*Outram 2002*). It is also important to note that the size fractions of the bones collected in the open areas were larger than those in the house, once again emphasising the idea of waste disposal from the house to the street.

On the road, two fragmented horn cores were found, showing cut marks made during the removal of the keratinous horn sheath and, therefore, a culinary uninteresting example of craft waste (the horn was used as a raw material) (see e.g., *Prummel 1978; Binford 1981; Lisowski 2014; Saliari, Felgenhauer-Schmidt 2017*). A bovine tibia, gnawed at both ends, was also found. The latter was thought to have been gnawed on by (probably) dogs. Lying in the open, such organic waste was clearly accessible to animals (see e.g., *Walters 1984; Pokines 2021*).

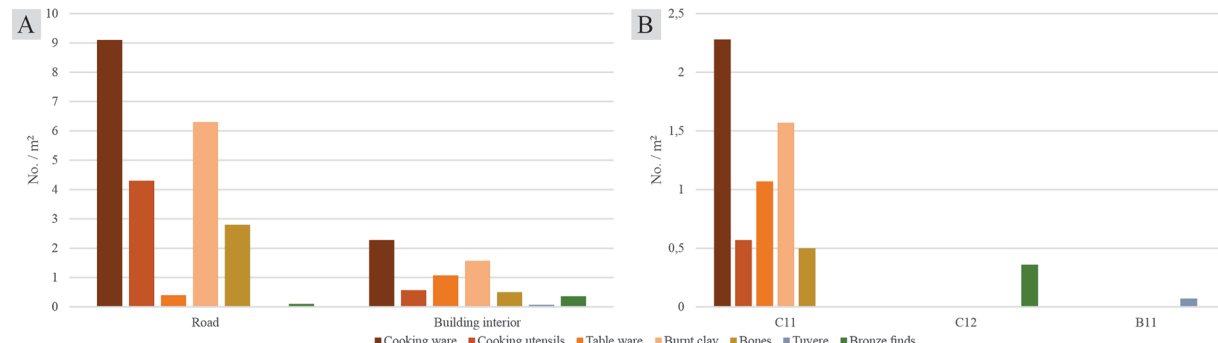


**Fig. 8. Pungrt hillfort. Comparison of macro-artefact densities between Building 24 interior and Road 1 and (B) between quadrants within the Building 24 in the IIb2 phase (figure by P. Vojaković).**

## Micro-artefact evidence

The sampling for the micro-refuse within Building 24 was carried out in Room A and the southern part of Room C, where the floors were well preserved, as well as also on a part of Road 1 adjacent to the building. The sampling, sample processing and examination followed procedures described in Luka Gruškovnjak *et al.* (2025).

Excluding numerous natural neoformations (e.g., iron-manganese (hydr)oxide nodules), the heavy fraction assemblage comprised 19 843 identified fragments in 2mm to >8mm size fractions and additional 599 magnetic pieces in 1–2mm size fraction. They were divided into five material groups (lithics, ceramics, lime, metallic, and faunal remains) (Tab. 3), further subdivided into 33 (sub)types. We separately examined the light fraction assemblage, acquired by flotation, which is comprised of charred botanical remains, representing the sixth material group (see Gruškovnjak *et al.* 2024.4.4).

### Micro-artefact SEM-EDS analysis

Several types or subtypes (see Tab. 3) have been analysed and defined using scanning electron microscopy (SEM) and energy dispersive X-ray spectroscopy (EDS) analysis (see Gruškovnjak *et al.* 2025), including fragments of metallurgical materials, lime and a lithic grain of graphite schist.

Metallurgical materials combine two main by-products of metallurgical processes: hammerscale and slag (Gruškovnjak *et al.* 2024.4). Both were further subdivided according to magnetism and various visual characteristics. Their interpretation and typology were established using SEM-EDS analysis. The subtypes of hammerscale include flakes of iron oxides produced

during forging and welding (Fig. 10.A–B); spheroids formed during welding or purifying the bloom (Fig. 10.C–D); and miscellaneous pieces with quartz sand flux produced during welding (Fig. 10.E–F). Hammer-scale is related to blacksmithing (see e.g., Dungworth, Wilkes 2007; 2009), while slag could also be related to iron smelting or copper metallurgy. Most slag pieces display black, greyish, and reddish colours; they have a porous structure and a typical solidification dendritic microstructure (Fig. 10.G–H). They are related to ferrous metallurgy, either smelting or the accumulation of clinker (mixture of inorganic impurities such as hammerscale, flux, ash, vitrified clay) in the smithing hearth (see e.g., Crew 1996; Serneels, Perret 2003; Miller, Killick 2004; Dunster, Dungworth 2012; Workman *et al.* 2021). In addition, two fragments display greenish to bluish colours, suggesting copper metallurgy, confirmed by the presence of Cu and Pb (Fig. 10.I) (see e.g., Eliyahu-Behar *et al.* 2012; Nerantzis *et al.* 2017).

Two types of lime were identified and analysed with SEM-EDS (Gruškovnjak *et al.* 2024.4.6.3). The EDS spectra (Fig. 11.A–B) corresponded with those reported for ancient calcitic mortars and lime plasters (e.g., Borsoi *et al.* 2019; Mignardi *et al.* 2021), confirming their identification. The first type had a pure white porous lime fabric with numerous medium to coarse sand sized rounded limestone or dolomite grains as aggregate. The second had an off-white, less- or non-porous fabric with numerous fine to medium sand sized angular and rare rounded limestone or dolomite grains. The comparison with floor sequences captured in thin sections (Ig 3–5, 94) suggests that the second type represent aggregates of either clay-lime plaster (SU 2064.2) or clay lime finishing coats and washes, such as those identified at Location 2 (SUs 2064.4, 2064.6, 2064.8). The higher values of Si and Al also

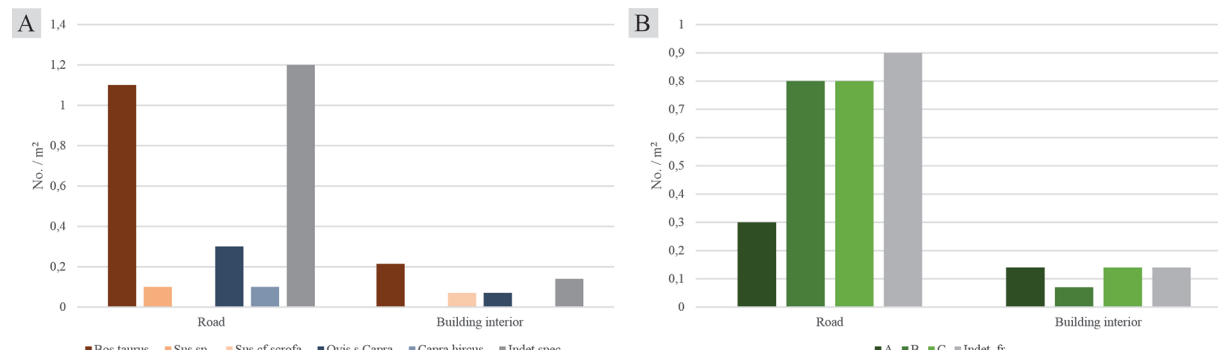


**Fig. 9. Pungrt hillfort. Comparison of macrofaunal remains from Building 24 and Road 1 in the IIb2 phase from the perspective of (A) species representation and (B) quality of meat (A: high, B: medium, C: low quality, after Uerpmann 1973) (figure by P. Vojaković).**

MATERIAL GROUP	TYPE	SUBTYPES	POSSIBLE INTERPRETATION	
LITHIC	Limestone and dolomite	Angular grains	Building material (roads, floors, lime etc.), environmental (background geology)	
		Rounded grains	Building material (lime, roads)	
	Sandstone and conglomerate	Lithic sandstone	Tools, implements, utensils	
		Micaceous sandstone with sericite-quartz matrix		
		Micaceous sandstone with calcite matrix		
		Quartz conglomerate		
		Chert pebbles		
	Other	Quartz crystals and grains	Raw material (metallurgy, pottery, floors)	
		Graphite schist	Raw material (pigment?)	
CERAMIC	Coarse pottery		Cooking ware, storage ware (?)	
	Fine pottery		Table ware, cooking utensils, tools and implements, building material	
	Daub		Building material (daub), burnt pottery	
	Burnt clay		Building material (floors, fire installations)	
	Vitrified and sintered clay	Red to black vitrified	Building material (fire installations), metallurgical tools	
		Yellow to brown vitrified		
		Sintered		
LIME	Lime type 1		Building material	
	Lime type 2		Building material (floors)	
METAL	Hammerscale	Magnetic / weakly-magnetic / non-magnetic	Blacksmithing (iron forging, welding, burning)	
		Flakes / spheroids / miscellaneous		
	Slag	Magnetic / weakly-magnetic / non-magnetic	Blacksmithing (clinker), iron smelting, copper metallurgy	
		Glassy / non-glassy		
		Iron / copper		
FAUNAL	Bone (mammals)	Unburnt		
		Burnt	Food processing, raw material	
		Carbonised	Fuel, casual burning (refuse), intentional burning (raw material)	
		Calcined		
	Bone (micromammals)			
	Bone (reptiles)			
BOTANICAL	Bone (fish)			
	Molluscs			
	Insects			
	Charcoal			
	Fruits and seeds			
	Cereal food			

**Tab. 3. Pungrt hillfort. A representation of material groups, types and subtypes of micro-artefacts discovered within Building 24 and on Road 1 in the IIb2 phase (figure by L. Gruškovnjak; for detailed descriptions see Gruškovnjak et al. (2024)).**

point to the mixing of lime with clay. On the other hand, the first type has no parallels in any material discovered in a context that would allow for its functional interpretation.

The lithic grain of graphite schist was black to dark grey in colour with very well-developed discontinuity planes (Fig. 11.C) and fine (< 2mm) spacing between cleavage planes. SEM-EDS analysis was used to further determine its structure and composition. In some cases, we observed 0.2mm wide openings filled with secondary minerals. Phaneritic grains of graphite up to 75 $\mu$ m in size were also observed (Fig. 11.D). The aphanitic groundmass consists of inosilicates (probably amphiboles), while the phaneritic mineral grains were identified as graphite (Fig. 11.E). The rock was named as graphite schist in accordance with the Systematics of Metamorphic Rocks (Fettes, Desmons 2007).

### **Micro-artefact radiocarbon dating**

Two radiocarbon samples were selected from among archaeobotanical material in micro-artefact assemblage to establish its absolute chronology (see *e.g.*, Teržan, Črešnar 2014:703), while a fragment of charred cereal food was dated to between 550 and 405 cal BC (76.8%; 2425 $\pm$ 24 BP; SUERC-123527) (Fig. 12). The two dates thus narrow the Late Hallstatt Phase IIb2 of Building 24 to the second half of the 6th century BC and the early 5th century BC.

### **Micro-artefact patterning**

Micro-artefact assemblages can be studied using various statistical and spatial analyses (*e.g.*, Sherwood

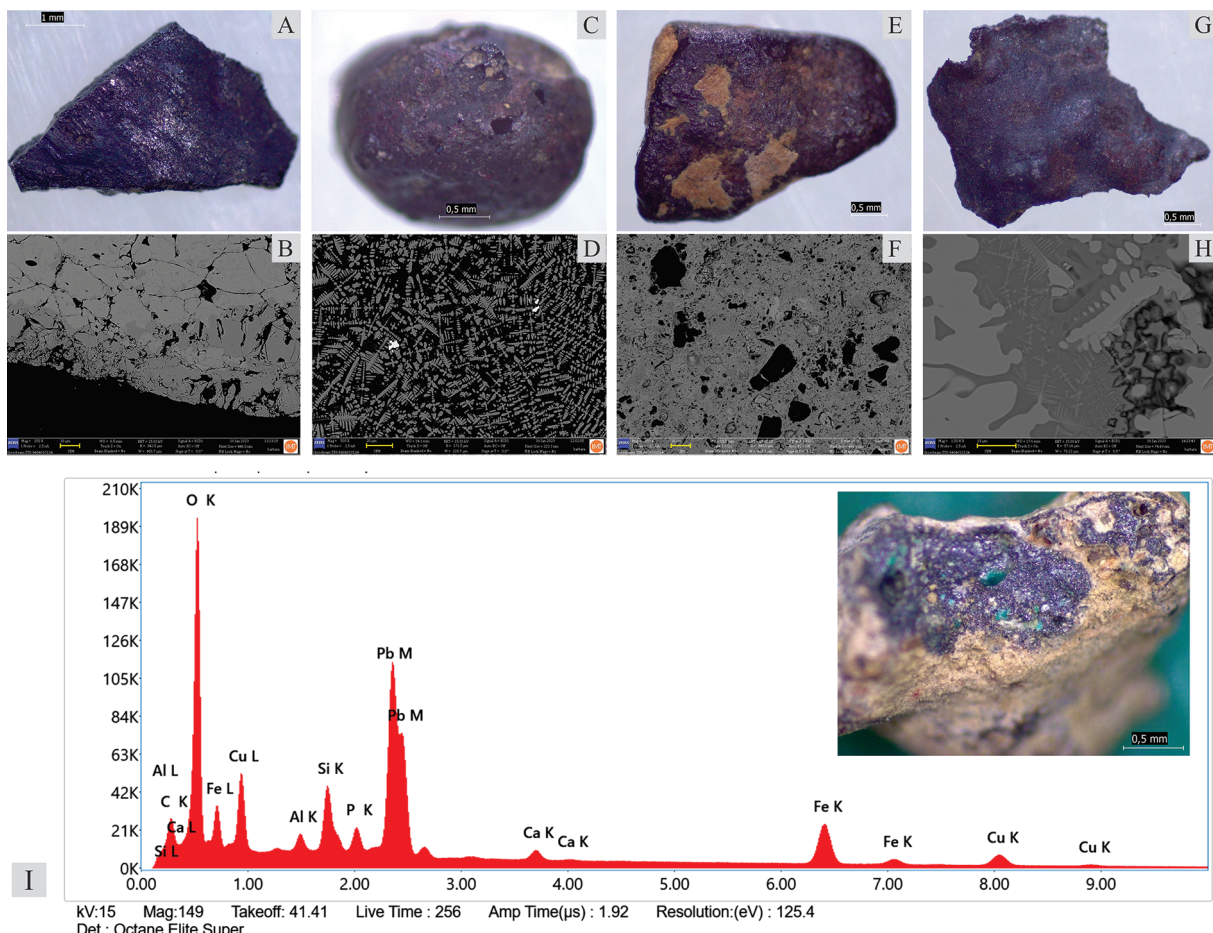


**Fig. 10. Pungrt hillfort. SEM-EDS analysis of micro-refuse from Building 24 in IIb2 phase. Flake hammerscale (A) photograph and (B) SEM image showing hammerscale with various ferrous oxides. Spheroid hammerscale (C) photograph and (D) SEM image showing dendritic microstructure typical for solidification. Miscellaneous hammerscale (E) photograph and (F) SEM image showing hammerscale, different ferrous oxides with flux. Slag (G) photograph and (H) SEM image showing solidification microstructure of slag. (I) Photograph of slag and EDS spectra showing presence of Pb and Cu, typical for copper smelting (figure by L. Gruškovič, J. Burja, B. Šetina Batič).**

2001; Kontogiorgos 2012; Ullah 2012; Milek, Roberts 2013; Ullah et al. 2014; Parker et al. 2018). Here, we primarily rely on a characterization study, the most straightforward analysis (see Parker et al. 2018), appropriate for gaining first insights into the micro- artefact assemblage and comparing it to the macro- artefact assemblage. To achieve this objective, we analyse the data mainly through densities<sup>2</sup> and concentrations<sup>3</sup> of individual categories of micro-refuse (see Gruškovič

et al. 2025). Densities were chosen for comparability to the macro-artefact data (Fig. 8) and concentrations for comparability between samples and different size fractions (Figs. 14.B, 15–17). In contrast to the macro- artefacts data, the high sampling resolution of micro- artefacts enables various meaningful spatial divisions of the building's interior, the most obvious being the distinction between Rooms A and C. Furthermore, it allows for a spatial distribution analysis,<sup>4</sup> offering a de-

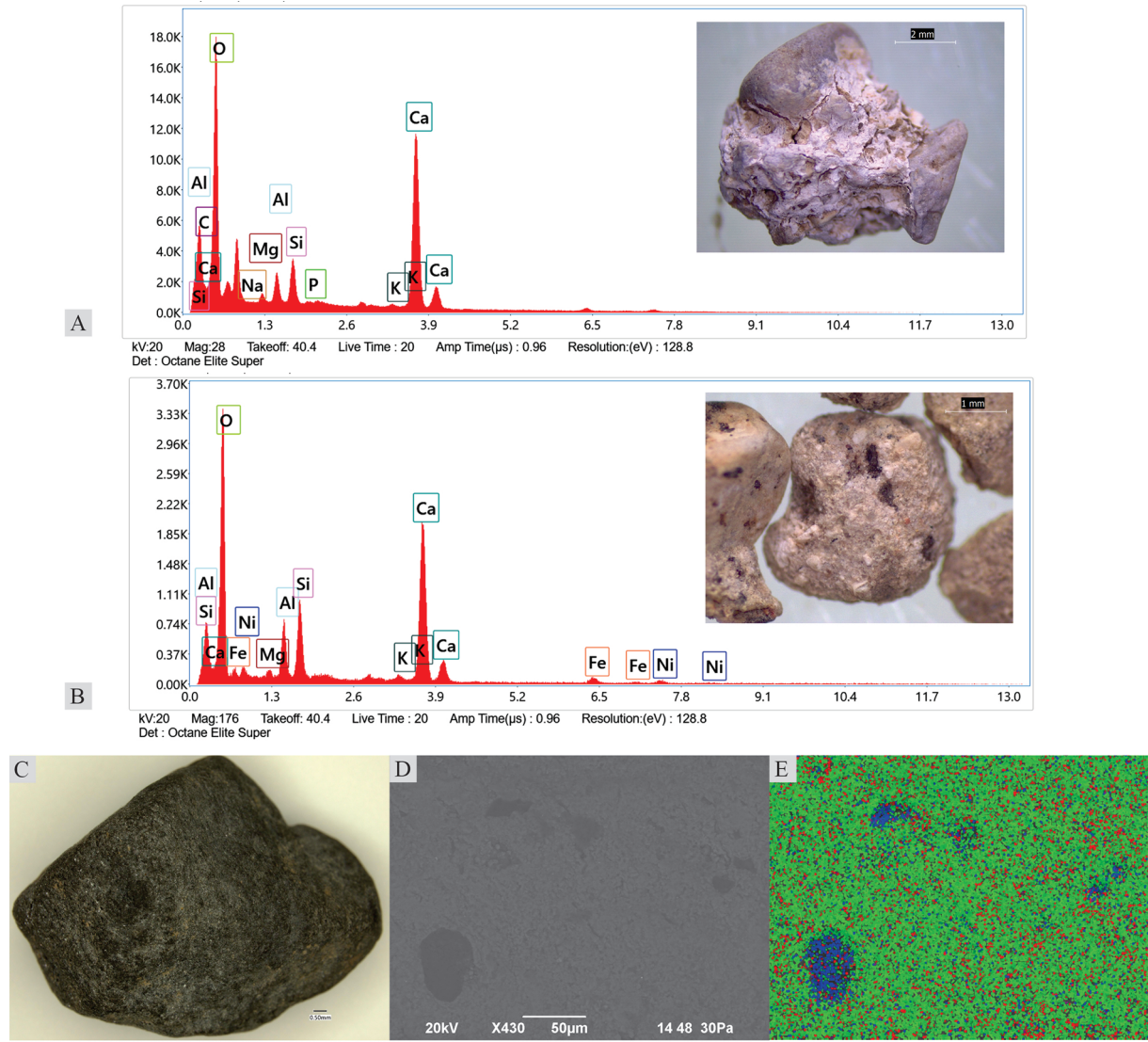


**Fig. 11. Pungrt hillfort. SEM-EDS analysis of micro-refuse from Building 24 in IIb2 phase. A a photograph and EDS spectra of lime type 1. B a photograph and EDS spectra of lime type 2. C macroscopic photograph of graphite schist, D SEM-EDS microphotograph showing phaneritic minerals of graphite and E element distribution of the sample (blue – carbon, green – silicon, red – aluminium), additionally containing also trace amounts of calcium, potassium and chlorine in aphanitic groundmass (figure by L. Gruškovič, B. Šetina Batić, R. Brajković).**

<sup>2</sup> The fragment counts from all size fractions of individual material types were added and calculated into the density per square metre.

<sup>3</sup> Concentrations per litre of sediment were calculated by dividing the fragment counts in each sample and size fraction by the bulk sample volume to ensure comparability between samples.

<sup>4</sup> To obtain high-resolution density plots we employed the kriging interpolation method in the Surfer software using concentrations of individual types of material.

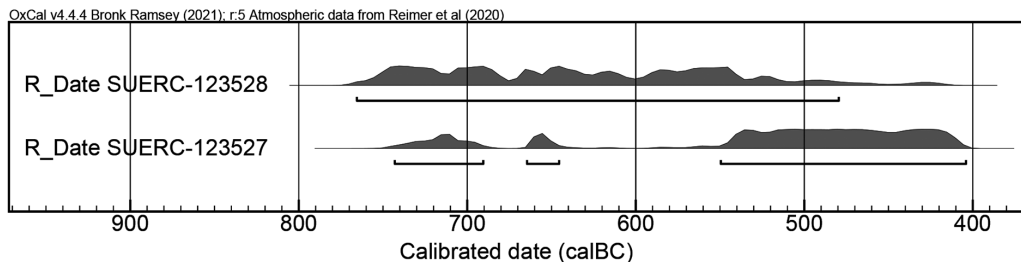


**Fig. 12. Pungrt hillfort. The cumulative diagram of micro-refuse radiocarbon dates from Building 24. SUERC-123528: carbonized wheat seed (*Triticum sp.*). SUERC-123527: carbonized cereal food (figure by T. Leskovar).**

tailed insight into the spatial structure of activities within the sampled area. Because a detailed spatial analysis of all documented materials in all size fractions goes beyond the scope of this paper, we focus only on three types, which are most relevant for the present discussion: hammerscale and both types of lime in the 2–4mm fraction (Fig. 18).

Based on previous research conducted on refuse behaviour, artefact fragmentation and micro-refuse, the interpretation of micro-artefacts patterning in the contexts of Building 24 and Road 1 in front of it was based on the following assumptions:

① In the case of intensive cleaning within the building, less material can be expected in its interior, especially in the case of larger size fractions. Only the finer size fractions will represent primary refuse and reflect long-term patterns of activities and their spatial structure within the building. In comparison, the larger size fractions will more likely reflect processes at the

time of abandonment. We can therefore expect a poor match between small and large size fractions (Hayden, Cannon 1983.156; Deal 1985.260,269; Dunnell, Stein 1989.37; Nielsen 1991.497,501; Tani 1995.234,244, 246,247; Sherwood et al. 1995.453; LaMotta, Schiffer 1999.21–22).

② In the case of intensive cleaning within the building, an increased amount of daily non-hazardous refuse can be expected on the adjacent road due to frequent floor sweeping and hearth cleaning. In such secondary refuse contexts we can expect a better match between small and large size fractions (Hayden, Cannon 1983.126–130; Deal 1985.261–262; Rosen 1989.566,573; Metcalfe, Heath 1990.782; Tani 1995.237, 239–240,244,247; Sherwood et al. 1995.453; LaMotta, Schiffer 1999.21–22).

③ For materials only or mainly represented in the building's interior, we can assume they are specific types of refuse (hazardous or valuable) associated with

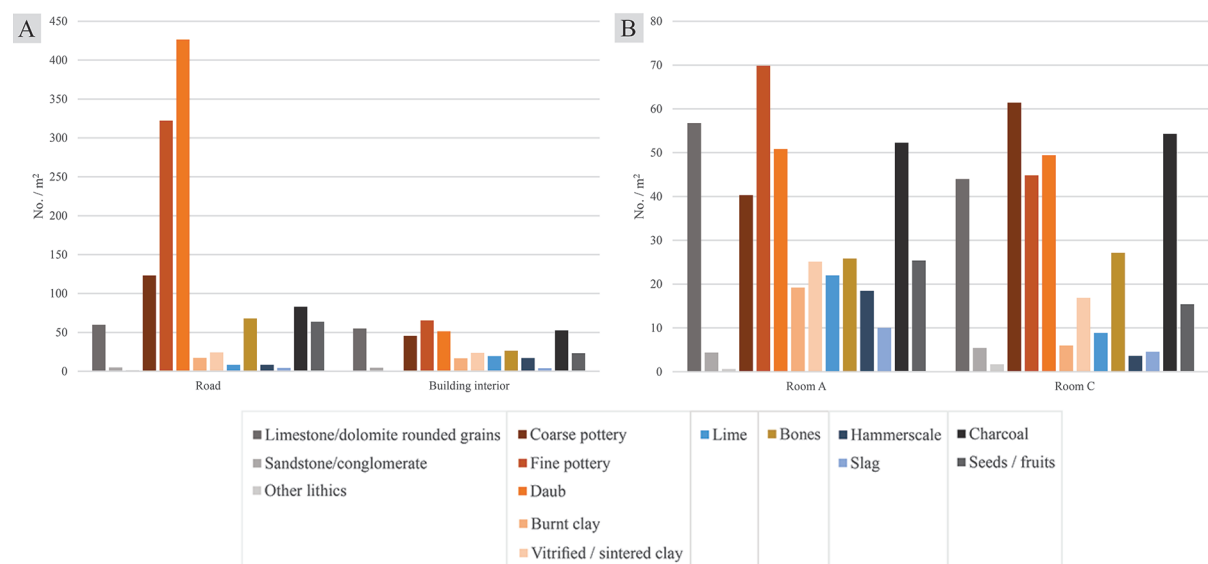


**Fig. 13. Pungrt hillfort. Comparison of micro-refuse densities (A) between the interior of Building 24 and Road 1 in the IIb2 phase and (B) between Rooms A and C within Building 24 in the IIb2 phase (figure by L. Gruškovnjak).**

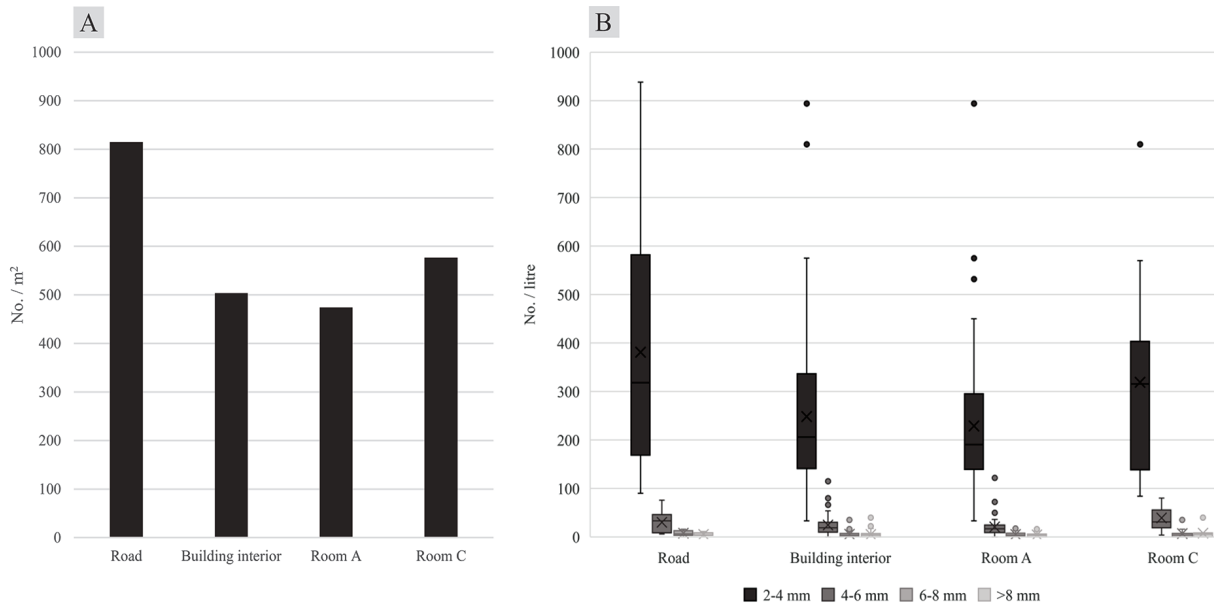


**Fig. 14. Pungrt hillfort. Comparison of (A) densities and (B) the distribution of concentration values of limestone/dolomite angular grains between the interior of Building 24 and Road 1 and between Rooms A and C within Building 24 in the IIb2 phase (figure by L. Gruškovič).**

activities within the building that require different management than ordinary refuse (Tani 1995.240; LaMotta, Schiffer 1999.21–22; Parker et al. 2018.69–70).

④ For materials only or mainly represented on the road, we can assume they were not related to the disposal of refuse from cleaning within the building but to activities and processes specific to the road (Parker et al. 2018.69–70) or other adjacent areas.

The regular cleaning of the building's interior was indicated by much higher densities and concentrations of various materials on the road compared to the building. Furthermore, we could observe the expected discrepancies between the size fractions within the building. Most of the material was represented as primary micro-refuse smaller than 6.3mm, and any larger fragments were present only as outliers (Figs. 13.A; 15).

The higher densities on the road could, on the one hand, indicate a secondary refuse context. The significantly higher densities of bones, charcoal, and burnt plant seeds and fruits can be interpreted mainly as domestic secondary refuse resulting from cleaning the building's interior and dumping the sweepings onto the road. A similar interpretation might be suggested for coarse pottery, fine pottery and daub, whose densities were exceptionally high. Compared to other materials, their concentrations on the road were high in all size fractions, probably indicating the disposal of larger fragments on the road and their subsequent frag-

mentation due to road traffic (see Gifford-Gonzalez et al. 1985; Nielsen 1991). On the other hand, the exceptionally high densities and concentrations of these three types of material, among which daub stands out in particular, could also be related to activities and processes specific to the road. As noted in the macro- artefact patterning, they were probably mainly related to the intentional deposition of these materials on the road to aid runoff (Rosen 1989.566,573; Raja, Sindbæk 2020.179).

Another type of material related to road maintenance is angular limestone and dolomite grains (Fig. 14). Compared to pottery and daub, their grain size distribution shows that they are not associated with fragmentation of larger clasts but with the intentional use of granule gravel (2–4mm; after Wentworth 1922) for metalling and maintaining the road, which was evident in the macro-stratigraphic observations. Interestingly, the granule gravel is also present in very high densities and concentrations in the building, where it could have been unintentionally transported on the soles of people entering from the road into the building. However, its density in the interior is more than four orders higher than the rest of the identified materials, and is similarly high in both the room facing the road (Room A) and the room further in the interior (Room C). This could suggest intentional use in floor maintenance, perhaps to improve friction and prevent slippery floors or more likely as aggregate in the two identified types of lime.

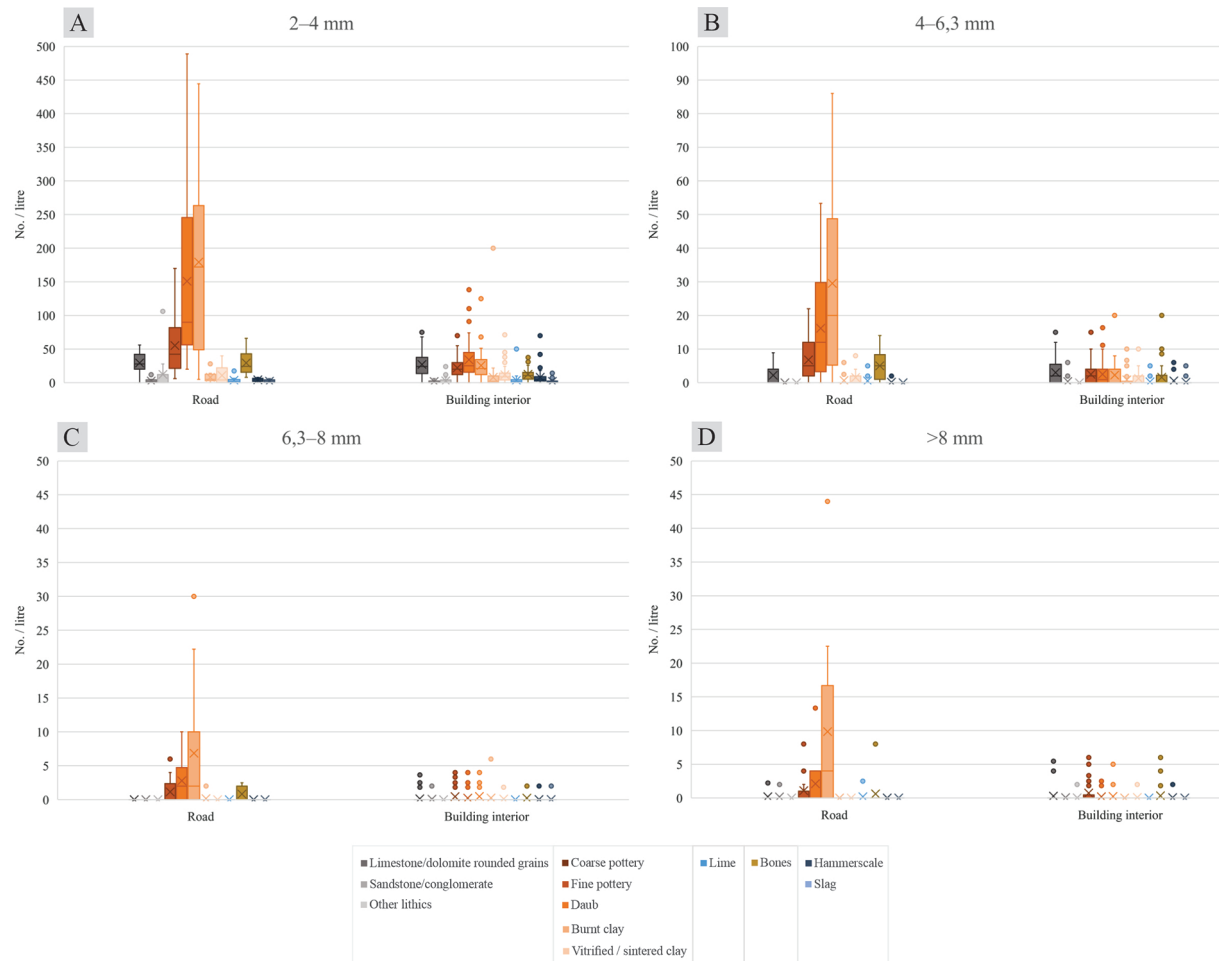


**Fig. 15. Pungrt hillfort. Comparison of micro-refuse concentrations between the interior of Building 24 and Road 1 in the IIb2 phase and between 2–4 mm, 4–6.3 mm, 6.3–8 mm, >8 mm size fractions by showing in detail the distribution of the concentration values (figure by L. Gruškovnjak).**

Lime and hammerscale represent materials particular to the building's interior, as evidenced by their distinctly higher densities and concentrations in the building (Figs. 13,15). Lime suggests a building material typical of building interiors, mainly floors, as demonstrated by the micromorphological analysis (see above), while hammerscale suggests blacksmithing (Starley 1995; Dungworth, Wilkes 2007; 2009) within the building and an activity typical of the interior. On the other hand, the density of slag, which is also related to metallurgical activities, was similar in the building and on the road. However, its concentrations within the building were higher. Burnt clay and vitrified and sintered clay display a similar trend. All three types of materials could be related to metallurgical activities within the building, namely to the use of a clay-lined smithing hearth and metallurgical utensils made of pottery (e.g., tuyeres and crucibles) and the production of clinker within the smithing hearth. Limestone and dolomite rounded grains, sandstone and conglomerate, and other lithics appeared also with

similar densities in both contexts but with somewhat higher concentrations within the building. Limestone and dolomite rounded grains are probably related to lime, while the sandstone and conglomerate pieces are probably associated with the use-wear of stone tools within the building. Because quartz is the most abundant material among the other lithics, this category mainly reflects its use as a raw material in the building, probably as flux in iron welding (see Fig. 10.F). The fact that hammerscale is the only activity-produced refuse which is distinctly more concentrated within the building suggests different waste management practices than other materials. It seems to have been collected separately and disposed of at another location, or perhaps even stored and intended for recycling (see Light 1984.62; Tani 1995.240; Thiele, Török 2022).

The comparison of micro-artefact patterning between the two rooms within the building revealed differences in their use (Figs. 13.B,16,17). The much higher densities and concentrations of hammerscale and slag in

Room A indicate that it would have functioned as a blacksmith's workshop where some bronze casting also took place (see Fig. 10.I). Among these materials, the interpretation of processes in which hammerscale is produced is the most straightforward, as this is a typical by-product of blacksmithing (iron forging, welding and burning) mainly produced in the 1–3mm size fraction (Starley 1995; Dungworth, Wilkes 2007; 2009). Indeed, it is the most abundant in the 1–2mm size fraction (Fig. 17) examined only for magnetic pieces, particularly for this reason. The grain size distribution showed that many pieces were also produced in the 2–4mm size fraction, but there were only a few larger pieces. Its spatial distribution shows two distinct concentrations in Room A (Fig. 18.A). Hammer-scale generally falls within 2m around the anvil (Dungworth, Wilkes 2009.37), and where the anvil or the blacksmith stood, the concentrations should be lower than immediately around it (Light 1984.59; Joutti Järvi 2009.980, Fig. 14). Therefore, we can reconstruct that the anvil and the blacksmith working it stood in be-

tween the two distinct concentrations in Room A (Fig. 18).

The higher densities and concentrations of fine pottery, burnt clay and vitrified and sintered clay in Room A suggest a relation to the blacksmithing, probably due to the use of clay-lined blacksmithing hearth and metallurgical pottery utensils. On the other hand, coarse pottery was present with much higher densities and concentrations in Room C. Because this type of primary refuse was related to the use of various cooking and storage ware, it suggests that the activities in Room C were more domestic. Somewhat higher concentrations of bone fragments would also point in this direction. The similar densities of charcoal in both rooms suggest the presence of hearths in both rooms, presumably a smithing hearth in Room A and a cooking hearth in Room C. Similarly, we may presume that the use of stone tools indicated by the presence of sandstone and conglomerate is related to the use of craft-related stone tools in Room A (e.g., anvil, polishers, whetstones) and

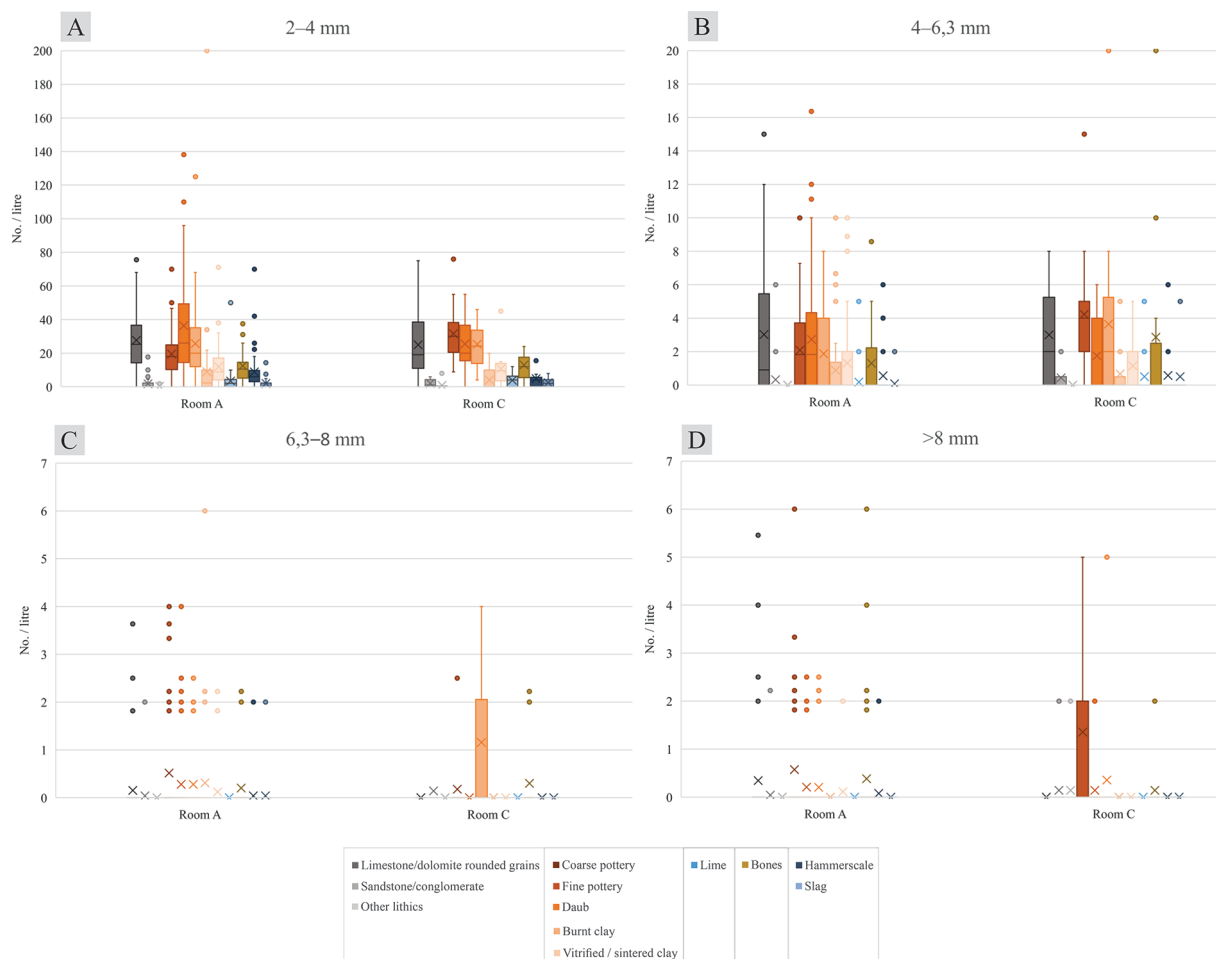


**Fig. 16. Pungrt hillfort. Comparison of concentrations between Rooms A and C within Building 24 in the IIb2 phase and between 2–4mm, 4–6.3mm, 6.3–8mm, >8mm size fractions by showing in detail the distribution of the concentration values (figure by L. Gruškovič).**

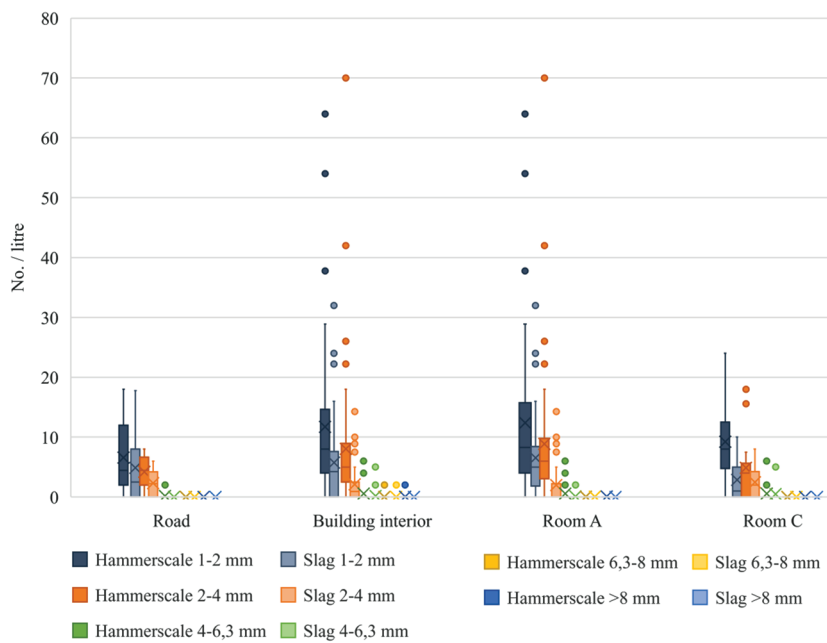


**Fig. 17. Pungrt hillfort. Comparison of concentrations of metallurgical remains between 1–2 mm, 2–4 mm, 4–6.3 mm, 6.3–8 mm, >8 mm size fractions within Building 24 and on Road 1 in the IIb2 phase (figure by L. Gruškovnjak).**

more domestic related tools in Room C (e.g., querns, pounders, whetstones). However, some activities related to food processing and preparation seem to have been performed in both rooms, as higher densities of charred seeds and fruits and relatively high densities and concentrations of coarse pottery and bone in Room A would suggest.

Lime as a building or floor maintenance material seems to have been used in a more considerable amount in the blacksmith's workshop in Room A. There, the distribution of lime type 2 (Fig. 11.B, 18. B) shows a distinct concentration around the vessel set into the floor, which corresponds to the lime plaster floors observed in the field and in thin section Ig 5 (SU 2064.2; Figs 3, 5; Tab. 1). The low-density areas may, on the one hand, be related to the unintentional spreading of this material across the room. On the other hand, they may be associated with the use of thin lime coats documented in thin sections Ig 3 and 4 (SU 2064.4,6,8; Figs 3, 5; Tab. 1). The generally low-density spread of lime type 1 (Fig. 11.A, 18. C) across the entire building could, therefore, be related to similar floor maintenance practices. However, these have been documented neither in the field nor in thin sections.

To conclude, the study of micro-refuse revealed functional differences between the two rooms examined in Building 24. Room A was used as a smithy, while Room

C was used for domestic activities. The interior of the building was regularly cleaned, leaving behind only micro-refuse, which escaped cleaning. This is evidenced by the grain size distribution of material, which suggests that activities are mainly reflected in the smallest size fractions examined while the information about activities diminishes with increasing size. The relationship between the information potential of individual size fractions is further demonstrated by summarising the number of material types and the number of fragments in individual size fractions (Tab. 4). The numbers of identified types and fragments are the highest in the 2–4 mm size fraction, which therefore holds most of the information about activities.

The number of types in the 4–6.3 mm size fraction drops slightly, but the number of fragments is significantly lower and considerably less informative for evaluating differences in activities between contexts. Moving to larger size fractions, the numbers of types and fragments drop substantially. In both 6.3–8 mm and >8 mm size fractions, around half of all identified types are not present anymore, and their numbers are negligible compared to smaller size fractions.

## Discussion

### ***The life cycle of Building 24***

The integrated data, obtained at the macro- and the microscopic scales, provide detailed insights into the Late Hallstatt phase IIb2 of the Building 24 (Fig. 2). Based on the chronology of the macro-artefacts (Fig. 7) and radiocarbon dating of micro-artefacts (Fig. 12), the building was dated to the late 6<sup>th</sup> century and early 5<sup>th</sup> century BC. When the house was built, the architectural remains of the preceding phase were levelled and employed, together with a mixture of various outdoor waste materials, as a preparation deposit, on which the new building was erected (SU 2071; Fig. 3.B). A low outer dry-stone foundation wall of roughly shaped limestone was laid down, and a timber building made in a cross-jointing technique was built upon it. Earthen material was used to fill the spaces between the beams,

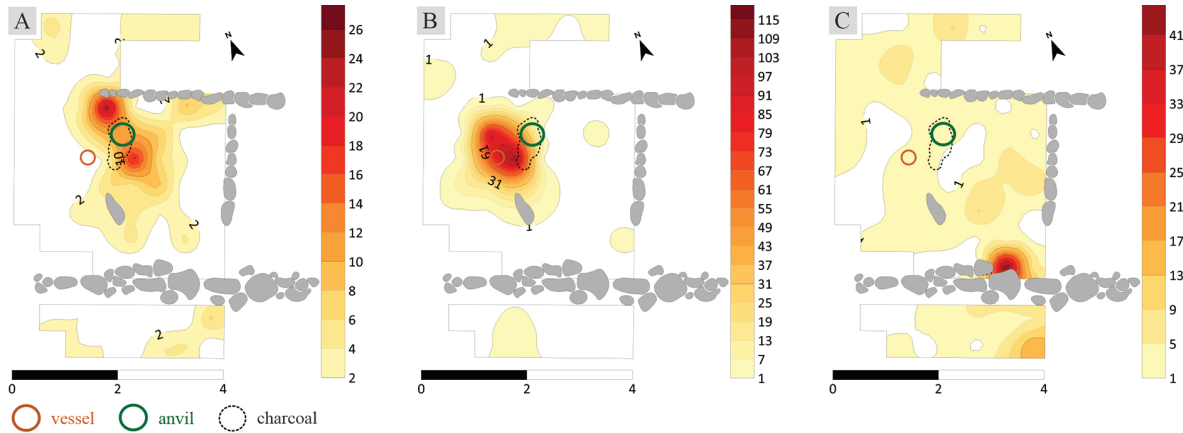


**Fig. 18. Pungrt hillfort. Distribution of hammerscale (A), lime type 2 (B) and lime type 1 (C) in 2–4mm size fraction within Building 24 and on Road 1 in the IIb2 phase (figure by L. Gruškovanjak).**

as indicated by the fragments of daub with beam impressions discovered across the site. The floor in the interior was constructed as some 9cm thick layer of yellowish-brown silty clay (SU 2064.1, Figs. 3,4,6). The foundations for thinner and lighter partition walls (e.g., wooden plank or wattle and daub construction), dividing the interior into three rooms, were laid down only after the floor was constructed.

Room A, facing Road 1, was used as a blacksmith's workshop, as evidenced by the concentration of hammerscale and slag in the micro-refuse (Figs. 13.B,16–17,18.A). The function of the adjacent Room B, where the floors were not preserved, remains unknown, while the northern Room C would have been mainly used for domestic purposes, as suggested by the higher concentrations of coarse pottery in the micro-refuse. The latter would have been related mainly to the cooking ware and, therefore, possibly food preparation (Figs. 13.B,16). Densities of charcoal and carbonized seeds and fruits in the micro-refuse light fraction (Fig. 13.B) suggest that fire installations, which were not uncovered during the excavation, would have probably been utilized as a smithing hearth in Room A, and as a domestic hearth in Room C.

In the blacksmith's workshop (Room A), a vessel (SF 2007; Fig. 7.14), probably serving as a quenching tub (see below), was set into the constructed floor (SU 2064.1), and the area surrounding it was plastered with clay lime (SU 2064.2; Figs. 3,5,18.B). The floor in the vicinity, where the anvil would have stood (Fig. 18.A), received a different treatment. Initially covered with a red clay coat (SU 2064.3; Figs. 3,5,6), it was subsequently cyclically maintained by skimming of its surface with alternating thin, earth- or lime-based coats and washes (SU 2064.4–9; Figs. 5,6).

During its use, the interior of the building was regularly cleaned and maintained, leaving behind only tiny pieces of primary refuse associated with a number of distinct activities within the building. These included various processes and activities associated with blacksmithing, as well as domestic activities primarily related to food processing and preparation. The waste materials produced in the process were mostly dumped on the road in front of the building with only a few notable exceptions. (Figs. 8.A,14.A,15). Hammerscale appears to be the main one, considering that it seems to have been collected separately from the remainder of the refuse, in order to be either recycled or disposed of at a different location. Furthermore, some types of refuse on the road, namely pottery and daub fragments, are possibly not only related to the dumping of waste from the building but, at the same time, also to road maintenance.

The end of the building's use-life might have been associated with the end of the life span of the building's construction materials and architectural elements, such as its timber frame, and constructed floors. We can assume a planned abandonment, as evidenced by the facts that its interior was thoroughly emptied ex-

Size Fraction	(Sub)types	Pieces
Macro-artefacts		320
Micro- artefacts	> 8 mm	321
	6,3–8 mm	341
	4–6,3 mm	1734
	2–4 mm	17447

**Tab. 4. Pungrt Hillfort. Comparison of the numbers of pieces and types or subtypes of materials discovered in various size fractions within Building 24 and on Road 1 in the IIb2 phase (figure by L. Gruškovanjak).**

cept for the vessel (SF 2007; Fig. 7.14) set into the floor in Room A, and some macro waste materials (pottery, burnt clay and bone), left behind in the same room (Figs. 7, 8.B). The area was then levelled again to prepare it for the rebuilding that followed, during the next phase IIc1.

### **Identification of floor construction and maintenance practices**

The on-site observation of floors provided the initial distinction between two different floor construction materials, which informed the subsequent micromorphological sampling; however, it failed to offer a more specific characterization of these or to detect any thinner and finer floor coats and washes. Micromorphology has proved, therefore, particularly important in examining the floor construction and maintenance practices, which reflected the temporal rhythms in the entangled life-cycles of the house and its inhabitants (see Boivin 2000; 2004; Prijatelj et al. *in prep.*).

Using micromorphological analysis, we identified two floor construction materials and four distinct floor skimming techniques employed in Building 24, during its Late Hallstatt phase IIb2. While the use of the first material – earth – has already been known from other Iron Age settlements in the region (e.g., Vojaković 2013; Svoljšak, Dular 2016), its microscale analysis has been lacking. Employing micromorphological analysis at Pungrt allowed for the identification of raw material provenance and distinct preparation techniques used in floor construction at the site. It was established that the yellowish-brown floor (SU 2064.1; Figs. 3,5) was made from the locally available, carbonate-free, and finely textured silty clay subsoils. These would have been wetted, kneaded, and pugged before being carefully packed, on top of the heterogeneous levelling fill, to form some 9cm thick layer, which would have been left to dry for several days.

In different areas of the house, the floor surfaces were skimmed with either plaster or various finishing coats and washes. The 6.5cm thick floor plaster (SU 2064.2; Figs. 3,4,18.B), identified exclusively in the wider area of the ceramic vessel (SF 2007; Fig. 7.14), was manufactured using lime-based technology. The stratigraphic observations at the macro- and micro-scales have revealed this to be a general pattern in the houses on the lowest terrace of the hillfort, with clay lime typically plastered across the constructed floors where the ceramic vessels were built-in. Pending the results of the micro-residue analysis of the vessels, it is possible that

the plastered areas required both a greater mechanical strength and a better heat and liquid resistivity compared to the constructed earthen floors. This was probably due to the distinct activities that occurred in these areas of the house. The micro-refuse data from Building 24 indicates that the plastered floor section was located near the anvil (Fig. 18.A–B), where all the blacksmithing processes that required the use of heavy tools and equipment, such as heating, forging and welding, were carried out. Significantly, a quenching tub would have been placed somewhere in the immediate vicinity of the anvil. Considering that these were typically simple containers, which may have been set into a pit (Light 1984.57–58), the ceramic vessel (SF 2007) built into the lime-plastered floor appears to have served such a function. Had the vessel indeed been employed as a container for the quenching liquid, the regular spillage of this may have necessitated the plastering of the earthen floor in this area with the material that was less susceptible to damage caused by the liquids. The thermal alterations of plaster, most intensively at its contact with the vessel and within the vessel's interior itself, further indicate a type of process associated with the high temperatures – possibly the process of quenching.

In contrast to constructed earthen floors, the manufacturing technology for various types of lime skim would have been more complex. The production of quicklime involved heating of calcareous rocks at temperatures ranging from 800 to 900°C for several hours or longer. Rather than preparing a putty (*i.e.* slaked lime) that would have matured for months, the unslaked lime was mixed with varying amounts of mineral subsoil, carbonate aggregate and a limited amount of water, which triggered the dry slaking of the quicklime (see also Henry, Stewart 2012; Hunnisett Snow 2016; Karkanas 2007; Prijatelj, Gruškovnjak 2024). In the following step, the dry ingredients were mixed with enough water to obtain a viscous mixture, which was applied across the constructed floor surrounding the built-in vessel (SF 2007) in Room A and allowed to set. Rendering tools were likely used in the process, due to the caustic and alkaline nature of hydrated lime.

The striking microstratigraphic sequence of seven finishing coats and washes on top of the constructed floor in the northern section of Room A (SUs 2064.3–9; Tab. 1, Figs. 3,5,6) suggests that the floor surfaces in this part of the building were scrupulously maintained. The renovations were undertaken using both earth- and lime-based construction materials, with a distinct

temporal rhythm in the use of different skims evidenced throughout the sequence. The earliest, some 11 mm thick finishing coat was made of pure red clay mixed with quartz sand (SU 2064.3; Figs. 3.A,5), with the layer in question representing a single use of this construction material throughout the entire IIb2 microstratigraphic floor sequence. The subsequent, progressively thinner coats and washes (SU 2064.4–2064.9; Fig. 5) consisted of either clay lime or silty clay loam.

The evidence for the cyclical skimming of the floor surface correlates with the area where the anvil would have stood (Figs. 2,18.A). This plastering routine may have been dictated by the wear and tear of the floor surface in this focal area of the blacksmith's workshop. However, the cyclical alteration between the earth- and lime-based skims could suggest additional ritual and symbolic significance as similar practices related to cyclically occurring festivities have been documented in ethnoarchaeological studies (e.g., Boivin 2000; 2004). In fact, ritual practices related to blacksmithing, a transformative, socially embedded, and symbolically charged activity (see e.g., Njoku 1991; Budd, Taylor 1995; Bergstøl 2002; Haaland et al. 2002; Haaland 2004; 2007/2008; Barndon 2005; Giles 2007; Wright 2019; Nión-Álvarez 2022), should probably be expected, especially in the area of the anvil, one of the most important and emblematic of the blacksmith's tools (e.g., Njoku 1991.207; Giles 2007.406; Haaland 2008.92).

Significantly, establishing the proximity of the micromorphological blocks to the probable location of the anvil and interpreting this micro-stratigraphic sequence in relation to blacksmithing was only possible by integrating the results of micromorphological and micro-artefact analyses. While the microscopic analysis of the vertical floor sequence is highly informative about the floor construction and maintenance practices on its own, it provides, in the particular case of the Pungrt site, only limited information about distinct activities, which leave an imprint across the floor surface (compare Milek, Roberts 2013.1863 for a contrasting conclusion on a site in a different environmental setting). In general, various types of micro-refuse, which are present in significant quantities across the horizontal floor plane, are rarely captured in vertical thin sections. Perhaps the most striking example of the disparity between these two micro-archaeological methods is provided in the case of micromorphological samples Ig 3 and 4. They were located in the area of

Room A with the highest concentration of hammerscale (Figs. 2,18.A), which was absent in thin sections. Notwithstanding the occasional occurrence of soot (e.g., SU 2064.3; *Gruškovnjak et al. 2024.Fig. 5.B*), suggesting the proximity of the fire installation, the floor surfaces appear 'clean' as so often observed in micromorphological analyses of house floors (e.g., *Karkanas, Efstratiou 2009; Matarazzo et al. 2010; Milek 2012*). This is due to two reasons. On the one hand, various effective cleaning techniques and refuse management strategies employed within the buildings tend to keep the floor surfaces clean. Even more importantly, however, the lack of micro-refuse material within thin sections tends to reflect the significantly different effectiveness in capturing micro-artefacts distributed across a surface with discrete versus continuous sampling, a methodological issue more commonly discussed in survey archaeology (e.g., *Miller 1989; Gruškovnjak 2017.53–55*).

To elaborate, each micromorphological sample represents a discrete point within a continuous horizontal plane of the examined floor surface and has, as such, a very low probability of capturing micro-artefacts distributed across that plane, while the horizontally continuous micro-refuse sampling is well suited for this purpose. Therefore, the absence of micro-refuse trampled into the floor surfaces in thin sections should not be interpreted as evidence of the absence of such remains or as an indication of a limited range of activities within the building (e.g., *Matarazzo et al. 2010.462*).

At the same time, it is important to note that the micromorphological sampling in the vertical plane offers in-depth information on the spatial and temporal relationships between the individual floor (micro) layers, which micro-refuse analysis cannot provide on its own. In the particular example of Building 24, micromorphology demonstrated the presence of (at least) seven consecutive (sub)millimetre-thick skims, which coated the silty clay floor in Room A. With such microlayers regularly going undetected in the field (as was also the case at Pungrt), and with currently available field methods unable to provide for the continuous micro-refuse sampling of thin finishing coats and washes, the micro-refuse assemblages inadvertently tend to provide information on various distinct activities within much coarser temporal frame, which homogenises the micro-artefact data across a number of the subsequent floor microlayers. Despite this currently unresolved methodological issue and

despite the discrepancy in the temporal resolution of the two analytical methods, we strongly advocate for the continuous sampling of the entire floor surfaces (in contrast to *Hodder, Cessford 2004*), in order to gain a distinct set of data which would have been unobtainable through the micromorphological sampling alone. In fact, we contend here that the integration of micromorphological (*i.e.* vertical) and micro-refuse (*i.e.* horizontal) sampling is necessary within the household and settlement archaeology, in order to obtain the optimal set of micro-archaeological data.

### ***Interpretations of household activities and the use of space***

A comparison of the macro- and micro-artefact assemblages has shown that the only *in situ* piece of the household inventory left within the building, *i.e.* the only piece of *de facto* refuse (*Schiffer 1996.89–97; LaMotta, Schiffer 1999.22*), was the ceramic vessel (SF 2007, Fig. 7.14) set into the floor in Room A (Fig. 2). Apart from this, the building's interior was practically devoid of any large artefacts or large pieces of refuse. Most of the discovered and identified materials in the building were smaller than 6.3mm, with the majority falling into the 2–4mm size fraction (Tab. 4), which is clear evidence of the regular cleaning of the building's interior. With all the larger pieces of refuse related to activities within it intentionally removed, only tiny fragments that escaped cleaning techniques and became trampled into the floor were left behind (*LaMotta, Schiffer 1999.21*). These tiny pieces represent residual primary refuse (see *Tani 1995.236*) produced by daily or regularly recurring activities within the building throughout its use life.

At the end of the building's use life, all large artefacts and pieces of equipment, except for the vessel set into the floor, would have been taken out of the house, as demonstrated, for example, by the comparison between the lithic macro- and micro-assemblages. Not a single stone artefact was present in the macro-assemblage (Fig. 8), while all the main types of stone tool raw materials documented elsewhere across the settlement were identified within the analysed micro-assemblage (Tab. 3), indicating that all the typical stone tool types were regularly used inside the building throughout its use-life.

In a similar vein, recurrently used materials and regularly occurring activities were reflected only in the micro-assemblage, while the macro-assemblage represented only refuse related to the very end of the

building's use when previously regular cleaning practices were no longer maintained and its interior was systematically emptied. The two temporal scales associated with the micro- and macro-assemblage are, therefore, very different, with the first reflecting the entire use-life of the building, and the second encapsulating only a short period related to its abandonment. This clearly demonstrates that using macro-artefact assemblages to identify activities within buildings and functionally evaluate them is highly problematic and may lead to erroneous interpretations (see *Tani 1995.244,247; LaMotta, Schiffer 1999*). It also points to the fact that macro-artefact and micro-artefact data are not as complementary as often suggested (see *Dunnell, Stein 1989.31; Sherwood et al. 1995.431; Sherwood 2001.328*).

In the present case, for example, the building would have been interpreted as purely domestic based on the macro-assemblage, when, in fact, a blacksmith's workshop operated within it. A sole piece of pottery, a fragment of a tuyere (Fig. 7.13) might have suggested blacksmithing. Regardless, a single artefact would not have sufficed on its own to unambiguously identify Room A as a blacksmith's workshop. On the one hand, tuyeres may have been used in either smithing or smelting and are therefore broadly related to both types of metallurgical activities (*e.g., Tylecote 1981*). On the other, the object suffers the same drawback as all other macro-artefacts recovered by reflecting only a short and atypical time at the end of the building's use.

Even in the rare case when the macro-artefact assemblage would have represented the primary refuse reflecting regularly recurring activities (*e.g.*, the ceramic vessel SF 2007), they would have provided information only about a limited range of these, given that some produce material traces only in the micro-artefact size range (see also *Dunnell, Stein 1989.33–34*). Hammerscale, fish scales, and archaeobotanical remains, for example, represent distinct finds produced by anthropogenic activities only at the micro-scale. Furthermore, the majority of environmental data, including micromammal, mollusc and insect remains, is also accessible only at the micro-level.

Further differences exist between the two datasets. The present analysis demonstrated that with the decreasing scale, the number of material types increases (Tab. 4). The increased heterogeneity can be attributed to at least two different factors. First, as larger heterogeneous materials break down into increasingly smaller

pieces, the variability within the original material causes its fragments to become progressively different (see *Dunell, Stein 1989.35*). At the micro-scale, they can no longer be recognized as belonging to the same heterogeneous material but become so different that they are identified and classified as discrete types. A distinct example of such fragmentation principle in Building 24 would have been provided by the clinker formed at the bottom of a smithing hearth, which could have potentially broken down into different types of slag and burnt, vitrified or sintered clay or even fine pottery and daub (see *e.g.*, *Crew 1996; Serneels, Perret 2003; Miller, Killick 2004; Dunster, Dungworth 2012; Workman et al. 2021*). Further examples of heterogeneous materials, which may regularly be classified into several discrete micro-refuse types, include pottery with temper in its fabric, which could break down into both pieces with or without evidence of temper. If the original vessel was secondarily burnt, some fragments might also display properties (lighter hues, chalky feel) used to define daub in the present assemblage. Another example would be an unthoroughly and unevenly burnt bone that could break into calcined, burnt and unburnt pieces within the micro-refuse assemblage.

Related to this challenge is the fact that artefact types, which are clearly recognizable at the macro-scale, are no longer identifiable at the micro-level. For example, the ceramic vessels, at the macro-scale, can be easily classified into discrete forms and types with distinct functions. At the micro-scale, however, their fragments can no longer be correlated to certain forms or types (see also *Dunell, Stein 1989.35*). With most types of pottery micro-refuse identified at the micro-scale, it is not even possible to know whether they originated from a vessel, tool, or utensil or whether they were related to some construction material (compare Tabs. 2 and 3). Similarly, bones at the macro-level are easily taxonomically and anatomically identified, while at the micro-scale, such identification is mostly impossible. Other finds, which are produced only at the micro-scale (*e.g.*, hammerscale, fish scales and archaeobotanical remains in the particular case of Building 24), however, do not face the same challenge and consequently allow for straightforward identification. This is especially true of archaeobotanical remains, which can be very efficiently identified regarding plant taxonomy and anatomy (see *Andrič et al. 2016.70–72; Gruškovnjak et al. in prep.*).

The third group of materials is preserved only at the micro-scale. Despite the challenges with relating them to the macro-scale, they have the advantage of providing information on activities and processes which would have otherwise gone unnoticed. Take two types of lime identified at the micro-scale, for example. With only one of them identified at a macro-scale (Figs. 11.A–B, 18.B–C), the microrefuse data provides evidence of at least two different lime-plaster recipes, as well as two different types of use of this material.

Due to the broader range of materials preserved at the micro-scale, the chances of discovering rare materials are higher. This is illustrated by a single piece of graphite schist (Fig. 11.C–E) identified in the micro-assemblage, a material entirely absent from the macro finds assemblage at the site. Consequently, the micro-evidence becomes even more significant, as it reveals the presence of an exotic raw material not available within the territory of modern Slovenia. A graphite-rich formation has been identified in the Tauern Window in the Austrian Central Eastern Alps and in the Ultrahelvetic Grestener Klippenzone along the northern edge of the Alps, outcropping north of Salzburg. This facies also extends into the Moravian Zone of the Bohemian Massif and is widespread in the Europe-derived Tisza and Dacia Mega-Units in the Pannonian region (*Schmid et al. 2020*). It is found closest to the Pungrt hillfort in Austrian Central Eastern Alps, south of Salzburg (*Pestal et al. 2009*), and in eastern Croatia (*Šinkovec, Krkalo 1994*). Therefore, the fragment of graphite schist discovered in Building 24 indicates long-distance trade with one of these areas. Given that the only currently known use of this raw material in the Early Iron Age in Slovenia was as a painting pigment in pottery production (see *e.g.*, *Grahek, Košir 2018*), it appears that the inhabitants of the Pungrt hillfort, specifically those in Building 24, would have possessed working knowledge of pigment preparation and its subsequent application. This evidence suggests that the black and red coated ware, discovered at the site, may be of local production rather than imported (see *Vojaković et al. 2024. Fig. 12.2*), or that the pigment may have been used for other, as yet undocumented purposes, such as painting on perishable materials. Alternatively, it might have served as a refractory material in metalworking contexts (*e.g.*, *Bayley, Rehren 2007.47*), though there is currently no direct evidence for such a practice. As a valuable consumable, graphite schist would have been treated differently from more common materials, which were intentionally discarded and make up the bulk of the

settlement's macro- artefact assemblage (*Hayden, Cannon 1983.130–131; Tani 1995.239–240*). Consequently, the likelihood of its preservation in the macro- record is slim.

Nevertheless, most types of micro-refuse are represented in much higher quantities than the graphite schist. Combined with the high-resolution sampling grid, it is precisely this quality that gives them a significant advantage against the macro- assemblage data (see *Dunnell, Stein 1989.36–37*). As illustrated by this paper, even a simple characterization study comparing the densities and concentrations of various micro-refuse types provides an important insight into the behaviour related to waste management practices, road maintenance and the differences in activities between the road, building interior and the two rooms. Most notably, it allowed us to identify Room A as a blacksmith's workshop (Figs. 13, 15–17). On the other hand, the kriging analysis of the hammerscale distribution, which helped us to identify the location of the anvil within the workshop (Fig. 18.A), demonstrates the micro-refuse potential for providing further detailed insights into the spatial structuring of activities within the building when more advanced analytical techniques are employed. In the next phase of our research, we will therefore seek to focus on reconstructing the structured use of space within Building 24, especially within the blacksmith's workshop, and deciphering the metallurgical processes and the technological knowledge used by the Early Iron Age blacksmiths at the Pungrt hillfort.

## Conclusions

The analysis and comparison of evidence preserved at the macro- and micro-scales in phase IIb2 of Building 24 at the Pungrt hillfort provided crucial insights into the distinct strengths and weaknesses of different scales of observation, as well as the two micro-archaeological methods employed.

The macro-stratigraphic observations offered the context for understanding the household on a human scale, enabling us to identify the building's construction techniques and its internal division into three rooms. These macro-scale observations also highlighted variations in colour and texture across the floor in Room A, which informed the design of micro-archaeological sampling techniques and provided a framework for contextualising their results.

The multiscalar analysis of stratigraphic and artefactual data revealed that the building's abandonment was planned and related to the need for rebuilding. During the abandonment, the building's interior was thoroughly emptied, except for the vessel built into the floor of Room A and some pieces of pottery, burnt clay and animal bone. The macro- artefact assemblage from the building, therefore, correlated to the very short abandonment period and was not informative about the structured activities during its use-life. Data about these were, on the other hand, preserved in the micro- artefact assemblage. While neither macro-stratigraphic nor macro- artefactual evidence would have allowed us to suggest anything else but basic domestic activities within the building, micro-refuse analysis clearly showed that Room A was used as a blacksmith's workshop, and Room C mainly for domestic activities. Furthermore, the spatial distribution of hammerscale within the building allowed us to pinpoint where the anvil, one of the most important pieces of blacksmith's equipment, would have stood. The blacksmithing, as well as other aspects of activities, were completely invisible and undetectable at the macro-scale. These findings have important implications for studying activities in ancient households in general, and particularly in houses with their abandonment and rebuilding planned, which seems to be the case for most buildings at the Pungrt hillfort. Importantly, they also revealed that the macro- and micro- artefact data sets, which tend to be associated with different stages in the life cycles of the examined buildings, are not as complementary as often suggested.

The micromorphological analysis of the building's floors correlated and explained distinct variations observed during the macro-stratigraphic observations, revealing different floor construction materials, manufacturing techniques, and maintenance strategies. Significantly, it exposed the micro-stratigraphic floor sequence of (at least) seven subsequent coats and washes on top of the constructed, silty clay floor that were undetectable during excavation. The rhythmic alterations of contrasting, white and red skims located near the anvil in the area that experienced the heaviest wear, and also held symbolic significance within the smithy, suggest a combination of practical and possibly symbolically driven choices in the selection of floor renovation materials.

The spatial correlation between the described micro-stratigraphic sequence and the anvil, however, could only be achieved through the integration of micromor-

phological and micro-refuse analyses. Micromorphology alone was insufficient to detect distinct daily activities within the building. This highlights a significant drawback of this micro-archaeological method, one that is not often discussed. A similar gap in such discussions was observed regarding the much coarser temporal resolution of micro-refuse data compared to the floor sequences captured in thin sections. By demonstrating the complementary nature of both micro-archaeological methods in the study of the Early Iron Age smithy at the Pungrt hillfort, we strongly advocate for the integration of these methods within settlement archaeology in general, and household archaeology in particular.

Using such an integrated approach at Pungrt revealed that two distinct types of lime were used within Building 24. One type was employed as a floor plaster and floor coat, while the use of the second remains unclear at present. The discovery of lime at the hillfort was arguably one of the most significant findings of this study, especially considering that prior to the geoarchaeological research at Pungrt, lime plaster technology had not been identified at any prehistoric site in Slovenia. Although traditionally associated with Roman colonization, the integrated micromorphological and micro-refuse data from Pungrt demonstrated that lime technology was already in use in the core area of the south-eastern Alpine region – in what is now Slovenia – during the Early Iron Age.

In summary, integrating interdisciplinary data at multiple scales has significantly enhanced our understanding of distinct floor sequences, and household activities in Building 24. However, the value of this evidence extends beyond providing insights into the precise nature of building and manufacturing technologies, floor maintenance strategies and blacksmithing processes, as it also deepens our understanding of how symbolic and ritual aspects of one smithy (and its associated household) may be manifested at the material level. Thinking about Building 24 and the numerous processes associated with its life-cycle as multi-scalar allowed for different themes to come into focus, depending upon the analytical lens applied. In doing so we gained access to both ephemeral acts – such as the possible ritual spreading of bright red clay coat across part of the floor surface, which would have occurred within the experiential time of one day or less – and processes spanning much lengthier time-scales, such as repetitive heating, forging, welding and quenching that left material traces on the floor surface and that may have been ongoing throughout the building's use-life. As cogently argued by John Robb and Timothy R. Pauketat (2013) in their discussion on scale and change in archaeological narratives about the past, history – in this case, the history of one Late Hallstatt smithy at the urban hillfort of Pungrt – was a multi-layered process that unfolded through different temporalities and relations.

#### *Data availability*

*The data used in the study is available online in the Repository of the University of Ljubljana (Gruškvnjak et al. 2024).*  
*Funding statement*

*We thank the Slovenian Research and Innovation Agency for funding this research (project grants J6-3126 to MC and Z6-60183 to LG and research and infrastructure programme grants P6-0247, P4-0085, P2-0050, P1-0025 and P6-0064). In addition, this research was partly funded by the Ministry of Culture of the Republic of Slovenia and carried out in the framework of the MATRES project, approved as part of the first (preparatory) phase for the preparation of large interdisciplinary projects of the University of Ljubljana, funded by the Slovenian Research Agency development pillar (ARIS, RSF-A).*

#### *Acknowledgements*

*We thank Saša Kos, formerly from the Geological Survey of Slovenia for her help in SEM measurements on graphite schist and Dimitrij Mlekuž Vrhovnik from the University of Ljubljana, Faculty of Arts, Department of Archaeology, for his suggestions on the spatial analysis approach.*

## References

Andrič M., Tolar T., Toškan B. 2016. *Okoljska arheologija in paleoekologija: palinologija, arheobotanika in arheozologija*. Založba ZRC. Ljubljana.  
<https://doi.org/10.3986/9789610503484>

Barndon R. 2005. Sparks of life: The concept of fire in iron working. *Current Swedish Archaeology* 13(1): 39–57.  
<https://doi.org/10.37718/CSA.2005.03>

Bayley J., Rehren T. 2007. Towards a functional and typological classification of crucibles. In S. La Niece, D. R. Hook, P. T. Craddock (eds.), *Metals and Mines: Studies in Archaeometallurgy*. Archetype Publications. British Museum. London: 46–55.

Bergstøl J. 2002. Iron technology and magic in Iron Age Norway. In B. S. Ottaway, E. C. Wager (eds.), *Metals and Society: Papers from a session held at the European Association of Archaeologists Sixth Annual Meeting in Lisbon 2000*. BAR International Series 1061. BAR Publishing. Oxford: 77–82.

Binford L. R. 1981. *Bones. Ancient myths and modern men*. Academic Press. San Diego, New York, Boston, London, Sydney, Tokio, Toronto.

Boivin N. 2000. Life rhythms and floor sequences: excavating time in rural Rajasthan and Neolithic Catalhoyuk. *World Archaeology* 31(3): 367–388.  
<https://doi.org/10.1080/00438240009696927>

2004. Geoarchaeology and the goddess Lakshmi. In N. Boivin, M. A. Owoc (eds.), *Soils, Stones and Symbols: Cultural Perceptions of the Mineral World*. Routledge. Oxon: 165–86.

Borsoi G., Santos Silva A., Menezes P., Candeias A., and Mirão J. 2019. Analytical characterization of ancient mortars from the archaeological roman site of Pisões (Beja, Portugal). *Construction and Building Materials* 204: 597–608.  
<https://doi.org/10.1016/j.conbuildmat.2019.01.233>

Budd P., Taylor T. 1995. The faerie smith meets the bronze industry: Magic versus science in the interpretation of prehistoric metal-making. *World Archaeology* 27(1): 133–143.  
<https://doi.org/10.1080/00438243.1995.9980297>

Buser S., Debeljak I. 1997. Lithiotid Bivalves in Slovenia and Their Mode of Life. *Geologija* 40(1): 11–64.  
<https://doi.org/10.5474/geologija.1997.001>

Courty M. A., Goldberg P., and Macphail R. 1989. *Soils and Micromorphology in Archaeology*. Cambridge University Press. Cambridge.

Crew P. 1996. Bloom refining and smithing slags and other residues. *Historical Metallurgy Society; Archaeological Datasheet 6*: 1–2.

Črešnar M. 2007. Leseni objekti v pozni prazgodovini. *AR* 7(2): 12–19.

Deal M. 1985. Household pottery disposal in the Maya highlands: An ethnoarchaeological interpretation. *Journal of Anthropological Archaeology* 4(4): 243–291.  
[https://doi.org/10.1016/0278-4165\(85\)90008-X](https://doi.org/10.1016/0278-4165(85)90008-X)

Djurić B., Gale L., and Brajković R. 2022. Limestone quarry at Podpeč near Ljubljana (Slovenia) and its products. *Arheološki vestnik* 73: 155–198.  
<https://doi.org/10.3986/AV.73.06>

Dozet S. 2009. Lower Jurassic carbonate succession between Predole and Mlačevje, Central Slovenia = Spodnjekarsko karbonatno zaporedje med Predolami in Mlačevim, osrednja Slovenija. *RMZ – Materials and Geoenvironment* 56(2): 164–193. <http://www.dlib.si/details/URN:NBN:SI:DOC-2YNYNFUC>

Dozet S., Strohmenger C. 2000. Podbukovška formacija, osrednja Slovenija = Podbukovje Formation, Central Slovenia. *Geologija* 43(2): 197–212.  
<http://www.dlib.si/details/URN:NBN:SI:DOC-P4PUQFDH>

Dular J. 1982. *Die Grabkeramik der älteren Eisenzeit in Slowenien*. Dela 1. razreda SAZU 23. Založba ZRC. Ljubljana.

2008. Prehistoric Building Techniques and their Terminology. *Annales. Series historia et sociologia* 18(2): 337–348.

Dungworth D., Wilkes R. 2007. *An Investigation of Hammerscale: Technology report*. Research Department Report Series no. 26/2007. English Heritage.

2009. Understanding hammerscale: the use of high-speed film and electron microscopy. *Historical Metallurgy* 43(1): 33–46.

Dunnell R. C., Stein J. K. 1989. Theoretical issues in the interpretation of microartifacts. *Geoarchaeology* 4(1): 31–41.  
<https://doi.org/10.1002/gea.3340040103>

Dunster J., Dungworth D. 2012. *Blacksmith's Fuel. The Analysis of Slags from Iron-Working*. Technology Report. Research Report Series no. 16-2012. English Heritage. York.  
<https://doi.org/10.5284/1037501>

Eliyahu-Behar A., Yahalom-Mack N., Shilstein S., +5 authors, and Weiner S. 2012. Iron and bronze production in Iron Age

IIA Philistia: New evidence from Tell es-Safi/Gath, Israel. *Journal of Archaeological Science* 39(2): 255–267. <https://doi.org/10.1016/j.jas.2011.09.002>

Fehon J. R., Scholtz S. C. 1978. A Conceptual Framework for the Study of Artifact Loss. *American Antiquity* 43(2) (*Contributions to Archaeological Method and Theory*): 271–273. <https://doi.org/10.2307/279250>

Fettes D. J., Desmons J., Árkai P., Brodie K., and Bryhni I. 2007. *Metamorphic rocks: A classification and glossary of terms*. Cambridge University Press.

Gale L. 2015. Microfacies characteristics of the Lower Jurassic lithiotid limestone from northern Adriatic Carbonate Platform (central Slovenia). *Geologija* 58(2): 121–138. <https://doi.org/10.5474/geologija.2015.010>

Gale L., Rožič B. 2024. Signs of crustal extension in Lower Jurassic carbonates from central Slovenia. *Geologija* 67(1): 25–40. <https://doi.org/10.5474/geologija.2024.002>

García-Suárez A., Matthews W., and Portillo M. 2021. Micro-morphology: exploring microcontextual traces of settled life at Çatalhöyük. In Hodder I. (ed.), *Peopling the landscape of Çatalhöyük: Reports from the 2009–2017 seasons*. British Institute of Archaeology at Ankara. London: 263–280.

Gifford-Gonzalez D. P., Damrosch D. B., Damrosch D. R., Pryor J., and Thunen R. L. 1985. The third dimension in site structure: an experiment in trampling and vertical dispersal. *American Antiquity* 50(4): 803–818. <https://doi.org/10.2307/280169>

Giles M. 2007. Making metal and forging relations: Iron-working in the British Iron Age. *Oxford Journal of Archaeology* 26(4): 395–413. <https://doi.org/10.1111/j.1468-0092.2007.00290.x>

Goláňová P. 2023. *Oppidum as an urban landscape. A multidisciplinary approach to the study of space organisation at Bibracte*. Bibracte.

Grahek L., Košir A. 2018. Scanning Electron Microscopy Analysis of the Pottery from the Settlement at Most na Soči. In J. Dular, S. Tecco Hvala (eds.), *The Iron Age Settlement at Most na Soči: Treaties*. Ljubljana. ZRC SAZU Press. Ljubljana: 307–320.

Gruškvnjak L. 2017. Arheološki površinski pregled – osnovni koncepti in problemi. *Arheo* 34: 23–77.

Gruškvnjak L., Prijatelj A., Vojaković P., +6 authors., and Črešnar M. 2024. From macro to micro archaeological approach in settlement archaeology: a case study of Early Iron Age smithy at the Pungrt hillfort (Central Slovenia): Research data underlying the paper. Repository of the University of Ljubljana. Available at: <https://repozitorij.uni-lj.si/IzpisGradiva.php?id=164943&lang=eng>

2025. Macro to micro stratigraphic and artefactual evidence from an Early Iron Age smithy at the Pungrt hillfort (Central Slovenia). *Journal of Open Archaeology Data: in press*. <https://doi.org/10.5334/joad.145>

Gruškvnjak L., Tolar T., Prijatelj A., Šetina Batič, B., Vojaković P., Grčman H., and Črešnar M. *Tracing Invisible Hearths and Daily Routines through Carbonized Plant Remains and Geochemical Signals in an Early Iron Age Smithy at Pungrt Hillfort, Slovenia*. Manuscript submitted for publication.

Guštin M. 1973. Cronologia del gruppo preistorico della Notranjska (Carniola Interna). *Arheološki vestnik* 24: 461–506.

1979. *Zu den Anfängen der Eisenzeit an der nördlichen Adria*. Catalogi et monographiae 17. Narodni muzej Slovenije. Ljubljana.

Haaland G., Haaland R., and Rijal S. 2002. The Social Life of Iron. A Cross-Cultural Study of Technological, Symbolic, and Social Aspects of Iron Making. *Anthropos* 97: 35–54.

Haaland R. 2004. Technology, transformation and symbolism: Ethnographic perspectives on European iron working. *Norwegian Archaeological Review* 37(1): 1–19. <https://doi.org/10.1080/00293650410001207>

2008. Say it in Iron: Symbols of transformation and reproduction in the European Iron Age. *Current Swedish Archaeology* 15–16(1): 91–110. <https://doi.org/10.37718/CSA.2008.06>

Hayden B., Cannon A. 1983. Where the garbage goes: Refuse disposal in the Maya Highlands. *Journal of Anthropological Archaeology* 2(2): 117–163. [https://doi.org/10.1016/0278-4165\(83\)90010-7](https://doi.org/10.1016/0278-4165(83)90010-7)

Henry A., Stewart D. 2012. *Practical Building Conservation: Mortars, Renders & Plasters*. Farnham: Ashgate.

Hodder I., Cessford C. 2004. Daily Practice and Social Memory at Çatalhöyük. *American Antiquity* 69(1): 17–40. <https://doi.org/10.2307/4128346>

Homsey-Messer L., Humkey K. 2016. Microartifact analysis and site formation of a Mississippian house floor at Wickliffe mounds, Kentucky. *Southeastern Archaeology* 35(1): 8–24. <https://doi.org/10.1179/2168472315Y.0000000010>

Howard J. 2017. *Anthropogenic Soils*. Springer.

Hunnisett Snow J. 2016. *Inform: Hot-mixed Lime Mortars*. Historic Scotland. Edinburgh.

Jouttiäärvi A. 2009. The shadow in the smithy. *Materials and Manufacturing Processes* 24(9): 975–980.  
<https://doi.org/10.1080/10426910902987176>

Karkanas P. 2007. Identification of lime plaster in prehistory using petrographic methods: A review and reconsideration of the data on the basis of experimental and case studies. *Geoarchaeology* 22(7): 775–796.  
<https://doi.org/10.1002/gea.20186>

2018. Microscopic deformation structures in archaeological contexts. *Geoarchaeology* 34(1): 15–29.

Karkanas P., Efstratiou N. 2009. Floor sequences in Neolithic Makri, Greece: Micromorphology reveals cycles of renovation. *Antiquity* 83(322): 955–967.  
<https://doi.org/10.1017/S0003598X00099270>

Karkanas P., Goldberg P. 2019. *Reconstructing archaeological sites: understanding the geoarchaeological matrix*. Wiley Blackwell. Edinburgh.

Kontogiorgos D. 2012. Reviewing Non-Linear Micro-artefacts' Structure. *The Open Anthropology Journal* 5: 6–9.

Leslie A. B., Hughes J. J. 2002. Binder microstructure in lime mortars: implications for the interpretation of analysis results. *Journal of Engineering Geology* 35: 257–263.

Light J. D. 1984. The Archaeological Investigation of Blacksmith Shops. *Industrial Archaeology* 10(1): 55–68.

Lisowski M. 2014. Hides and horn sheaths: A case study of processed skulls and horn cores from the Early-Middle Neolithic site of Kopydłowo 6, Poland. *Assemblage PZAF* (2014): 32–41.

Lokier S. W., Al Junaibi M. 2016. The petrographic description of carbonate facies: are we all speaking the same language? *Sedimentology* 63(7): 1843–1885.  
<https://doi.org/10.1111/sed.12293>

Matarazzo T., Berna F., and Goldberg P. 2010. Occupation surfaces sealed by the Avellino eruption of Vesuvius at the early bronze age village of Afragola in southern Italy: A micromorphological analysis. *Geoarchaeology* 25(4): 437–466. <https://doi.org/10.1002/gea.20319>

Matthews W. 2005. Life-cycle and life-course of buildings. In I. Hodder (ed.), *Catalhöyük Perspectives: Reports from the 1995–99 seasons*. McDonald Institute for Archaeological Research: 125–150. Cambridge.

2017. Tells. In A. S. Gilbert (ed.), *Encyclopedia of Geoarchaeology*. Encyclopedia of Earth Sciences Series. Springer. Dordrecht: 951–972.  
[https://doi.org/10.1007/978-1-4020-4409-0\\_148](https://doi.org/10.1007/978-1-4020-4409-0_148)

Mignardi S., De Vito C., Botticelli M., +4 authors, and Medeghini L. 2021. Lime production in the late chalcolithic period: The case of Arslantepe (eastern Anatolia). *Heritage* 4(1): 91–104. <https://doi.org/10.3390/heritage4010005>

Milek K. B. 2012. Floor formation processes and the interpretation of site activity areas: An ethnoarchaeological study of turf buildings at Thverá, northeast Iceland. *Journal of Anthropological Archaeology* 31(2): 119–137.  
<https://doi.org/10.1016/j.jaa.2011.11.001>

Milek K. B., Roberts H. M. 2013. Integrated geoarchaeological methods for the determination of site activity areas: a study of a Viking Age house in Reykjavík, Iceland. *Journal of Archaeological Science* 40: 1845–1865.  
<https://doi.org/10.1016/j.jas.2013.02.001>

Milek K., Zori D., Connors C., Baier W., Baker K., and Byock J. 2014. Interpreting Social Space and Social Status in the Viking Age House at Hrísbrú Using Integrated Geoarchaeological and Microrefuse Analyses. In J. Byock, D. Zori (eds.), *Viking Archaeology in Iceland. Mosfell Archaeological Project*. Brepols: 143–162.

Miller C. L. 1989. Evaluating the Effectiveness of Archaeological Surveys. *Ontario Archaeology* 49: 3–12. <http://www.ontarioarchaeology.on.ca/publications/pdf/oa49-1-miller.pdf>

Miller D., Killick D. 2004. Slag identification at Southern African archaeological sites. *Journal of African Archaeology* 2(1): 23–47. <https://doi.org/10.3213/1612-1651-10017>

Mohammadi S. P., Horák J., Lisá L., Grytz J., Grison H., Bajer A., and Šmejda L. 2023. Soils as an environmental record of changes between Iron Age and Medieval occupations at Chotěbuz-Podobora hillfort. *Geoderma* 429: 116259.  
<https://doi.org/10.1016/j.geoderma.2022.116259>

Nerantzis N., Sanidas G., Jagou B., Kozelj T., and Panoussi K. 2017. An Archaic metallurgical workshop in Thasos (Greece): the case of Charitopoulos plot. *Science and Technology of Archaeological Research* 3(2): 148–160.  
<https://doi.org/10.1080/20548923.2017.1419659>

Nicosia C., Stoops G. (eds.) 2017. *Archaeological Soil and Sediment Micromorphology*. Wiley Blackwell. Hoboken.

Nielsen A. E. 1991. Trampling the Archaeological Record: An Experimental Study. *American Antiquity* 56(3): 483–503.  
<https://doi.org/10.2307/280897>

Níon-Álvarez S. 2022. The Metalworker as Social Agent: A longue durée Approach from Northwestern Iberia Atlantic Façade (Ninth-First Centuries BCE). *Cambridge Archaeological Journal* 32(3): 489–506.  
<https://doi.org/10.1017/S0959774321000615>

Njoku O. N. 1991. Magic, Religion and Iron Technology in Precolonial North-Western Igboiland. *Journal of Religion in Africa* 21(3): 194–215.

Ogrin M. 1998. Trortasta fibula v Sloveniji. *Arheološki vestnik* 49: 101–132.

Outram A. K. 2002. Bone Fracture and Within-bone Nutrients: an Experimentally Based Method for Investigating Levels of Marrow Extraction. In P. Miracle, N. Milner (eds.), *Consuming Passions and Patterns of Consumption*. Cambridge: 51–64.

Parker B. J., Prieto G., and Osores C. 2018. Methodological advances in household archaeology: an application of microartifact analysis at Pampa La Cruz, Huanchaco, Peru. *Ñawpa Pacha* 38(1): 57–75.  
<https://doi.org/10.1080/00776297.2018.1465381>

Pestal G., Hejl E., Braunstingl R., and Schuster R. 2009. *Erläuterungen Geologische Karte von Salzburg 1: 200'000*. Land Salzburg & Geologische Bundesanstalt.

Pokines J. T. 2021. Faunal Dispersal, Reconcentration, and Gnawing Damage to Bone in Terrestrial Environments. In J. T. Pokines, E. N. L'Abbe, and S. A. Symes (eds.), *Manual in Forensic Taphonomy*. CRC Press. Boca Raton, London New York: 201–248.

Prijatelj A., Gruškvnjak, L. 2023. Mikromorfološka preiskava organo-mineralnega zaporedja plasti v notranjosti gradu na Kašči. In A. Gaspari, A. Vičar (eds.), »...alle drew purchstal«: arheološke raziskave gradov vitezov Hertenberških na območju Jeterbenka nad Medvodami. *Documenta Archaeologica* 1. Znanstvena založba Filozofske fakultete. Ljubljana: 248–278. <https://doi.org/10.4312/9789612971014>

Prijatelj A., Gruškvnjak L., Vojaković P., Mušič B., Grčman H., and Črešnar M. 2024. Proto-urban hillfort at 10 microns: integrated geoarchaeological research at Pungrt (central Slovenia). *Antiquity* 98 (397), e4: 1–9.  
<https://doi.org/10.15184/ajy.2023.196>

Prijatelj A., Milek K., Gruškvnjak L., +4 authors, and Grčman H. *Floor construction technologies and maintenance strategies in the prehistoric household: integrating high-resolution geoarchaeological methods at the Early Iron Age urban hillfort of Pungrt, Central Slovenia*. Manuscript in preparation.

Prummel W. 1978. Animal bones from tannery pits of 's-Hertogenbosch. *Berichten van de Rijksdienst voor het Oudheidkundig Bondemonderzoek* 28: 399–422.

Raja R., Sindbæk S. M. 2020. Urban Networks and High-Definition Narratives. Rethinking the Archaeology of Urbanism. *Journal of Urban Archaeology* 2: 173–186.  
<https://doi.org/10.1484/JJUA.5.121535>

Robb J. E., Pauketat T. R. 2013. From moments to millennia: theorising scale and change in human history. In J. E. Robb, T. R. Pauketat (eds.), *Big Histories, Human Lives: Tackling the problem of scale in archaeology*. SAR Press. Sante Fe (NM): 3–33.

Rosen A. M. 1989. Ancient Town and City Sites: A View from the Microscope. *American Antiquity* 54(3): 564–578.  
<https://doi.org/10.2307/280783>

Saliari K., Felgenhauer-Schmiedt S. 2017. Skin, leather, and fur may have disappeared, but bones remain... The case study of the 10th century AD fortified settlement Sand in Lower Austria. *Annalen des naturhistorischen Museums in Wien, Serie A* 119: 95–114.

Schmid S. M., Fügenschuh B., Kounov A., +8 authors, and van Hinsbergen D. J. J. 2020. Tectonic units of the Alpine collision zone between Eastern Alps and western Turkey. *Gondwana Research* 78: 308–374.  
<https://doi.org/10.1016/j.gr.2019.07.005>

Seetah K. 2019. *Humans, animals, and the craft of slaughter in archaeo-historic societies*. Cambridge University Press. Cambridge.

Serneels V., Perret S. 2003. Quantification of Smithing Activities Based on the Investigation of Slag and Other Material Remains. In *Archaeometallurgy in Europe – Proceedings of the International Conference (Milan, Italy, 24–26 September 2003)*, Vol. 1. Associazione Italiana di Metallurgia. Milano: 469–478.

Sharples N. M. 1991. *Maiden Castle. Excavations and field survey 1985–6*. Archaeological Report no 19. English heritage. 1991. Swindon. [https://archaeologydataservice.ac.uk/archiveDS/archiveDownload?t=arch-1416-1/dissemination/pdf/9781848021679\\_all.pdf](https://archaeologydataservice.ac.uk/archiveDS/archiveDownload?t=arch-1416-1/dissemination/pdf/9781848021679_all.pdf)

Sherwood S. C. 2001. Microartifacts. In P. Goldberg, V. T. Holliday, and C. R. Ferring (eds.), *Earth Sciences and Archaeology*. Springer Science+Business Media. New York: 327–351.

Sherwood S. C., Simek J. F., and Polhemus R. R. 1995. Artifact size and spatial process: Macro- and microartifacts in a mississippian house. *Geoarchaeology* 10(6): 429–455.  
<https://doi.org/10.1002/gea.3340100603>

Starley D. 1995. Hammerscale. *Historical Metallurgy Society Datasheet* 10: 1–2. <http://scholar.google.com/scholar?hl=en&btnG=Search&q=intitle:Hammerscale#0>

Stoops G. 2021. *Guidelines for Analysis and Description of Soil and Regolith Thin Sections* (2<sup>nd</sup> edition). Soil Science Society of America. Wiley. Madison.

Šinkovec B., Krkalo E. 1994. Graphite deposits from Mt. Psunj in Slavonia (Eastern Croatia). *Geologia Croatica* 47(1): 117–126. <https://doi.org/10.4154/GC.1994.09>

Tani M. 1995. Beyond the identification of formation processes: behavioural inference based on traces left by cultural formation processes. *Journal of Archaeological Method and Theory* 2(3): 231–252.  
<https://doi.org/10.1007/BF02229008>

Tecco Hvala S. 2014. Early Iron Age ceramic situlae from Slovenia. In S. Tecco Hvala (ed.), *Studia praehistorica in honorem Janez Dular*. Opera Instituti Archaeologici Sloveniae 30. Založba ZRC. Ljubljana: 323–339.

Teržan B., Črešnar M. 2014. Attempt at an Absolute Dating of the Early Iron Age in Slovenia. In B. Teržan, M. Črešnar (eds.), *Absolute Dating of the Bronze Age and Iron Ages in Slovenia*. Catalogi et monographiae 40. Ljubljana: 703–724.

Teržan B., Trampuž N. 1973. Contributo alla cronologia del gruppo preistorico di Santa Lucia. *Arheološki vestnik* 24: 416–460.

Thiele Á., Török, B. 2022. A possible medieval recycling technique – smelting iron using hammerscale. *IOP Conference Series: Materials Science and Engineering* 1246(1): 012008. <https://doi.org/10.1088/1757-899x/1246/1/012008>

Tylecote R. F. 1981. From pot bellows to tuyeres. *Levant* 13 (1): 107–118. <https://doi.org/10.1179/lev.1981.13.1.107>

Uerpmann H.-P. 1973. Animal bone finds and economic archaeology: A critical study of ‘ostearchaeological’ method. *World Archaeology* 4(3): 307–322.  
<https://doi.org/10.1080/00438243.1973.9979541>

Ullah I. I. T. 2012. Particles of the Past: Microarchaeological Spatial Analysis of Ancient House Floors. In B. J. Parker, C. P. Foster (eds.), *New Perspectives on Household Archaeology*. Eisenbrauns. Winona Lake (IN): 123–138.

Ullah I. I., Duffy P. R., and Banning E. B. 2014. Modernizing Spatial Micro-Refuse Analysis: New Methods for Collecting, Analyzing, and Interpreting the Spatial Patterning of Micro-Refuse from House-Floor Contexts. *Journal of Archaeological Method and Theory* 21(3): 1238–1262.  
<https://doi.org/10.1007/s10816-014-9223-x>

Urleb M. 1974. *Hallstattzeitliches Gräberfeld Križna gora*. Catalogi et monographiae 11. Narodni muzej Slovenije. Ljubljana.

Vidic N. J., Prus T., Grčman H., +8 authors, and Lobnik F. 2015. *Tla Slovenije s pedološko kartou v merilu 1:250 000/ Soils of Slovenia with soil map 1:250 000*. In H. Grčman, N. J. Vidic, M. Zupan, F. Lobnik, A. Jones, and L. Montanarella (eds.), *Tla Slovenije s pedološko kartou v merilu 1: 250 000/ Soils of Slovenia with soil map 1:250 000*. European Commission Joint Research Center (JRC). Publication Office of the European Union. Ljubljana. <https://op.europa.eu/en/publication-detail/-/publication/538dee5b-dfbf-45d6-be3c-d4b6fab3110d/language-en>

Vojaković P. 2013. *Prazgodovinska Emona. Novo odkrita protourbana naselbina na Prulah in njeno mesto v času in prostoru*. Unpublished PhD dissertation. Universitiy of Ljubljana. Faculty of Arts. Ljubljana.

Vojaković P., Gruškovič L., Prijatelj A., Mušič B., Horn, B., and Črešnar M. 2024. Early Iron Age urbanism in the south-eastern Alpine region: a case study of the Pungrt hillfort (Central Slovenia). *Documenta Praehistorica* 51: 490–519.  
<https://doi.org/10.4312/dp.51.25>

Walters I. 1984. Gone to the Dogs: a Study of Bone Attrition at a Central Australian Campsite. *Mankind* 14(5): 389–400.

Weiner S. 2010. *Microarchaeology: beyond the visible archaeological record*. Cambridge University Press. Cambridge.

Wentworth C. K. 1922. A Scale of Grade and Class Terms for Clastic Sediments. *Journal of Geology* 30(5): 377–392.  
<http://www.jstor.org/stable/30063207>

Workman V., Maeir A. M., and Eliyahu-Behar A. 2021. In search of the invisible hearth: An experimental perspective on early Levantine iron production. *Journal of Archaeological Science: Reports* 36: 102803.  
<https://doi.org/10.1016/j.jasrep.2021.102803>

Wright D. W. 2019. Crafters of Kingship: Smiths, Elite Power, and Gender in Early Medieval Europe. *Medieval Archaeology* 63(2): 271–297.  
<https://doi.org/10.1080/00766097.2019.1670922>

Žvab Rožič P., Rožič B., Gale L., and Brajkovič R. 2022. Provenance analysis of Roman limestone artefacts from Colonia Iulia Emona (Marof archaeological site, Slovenia). *Archaeometry* 64(5): 1057–1078.  
<https://doi.org/10.1111/arcm.12771>